University “Mediterranea” of Reggio Calabria
AGRARIA Department

Ph.D. course in Agricultural, Food and Forestry Sciences - Cycle XXXII
Curriculum Forestry Sciences

EFFECTS OF GRADE CONTROL STRUCTURES ON CHANNEL EVOLUTION IN SANDY TORRENT BEDS: A LABORATORY STUDY

DSS: AGR/08

Ph.D candidate
Antonino LABATE

Supervisor
Prof. Paolo PORTO

Ph.D. Coordinator
Prof. Marco Poiana

ACADEMIC YEARS 2016 - 2019

Effects of grade-control structures on channel evolution in sandy torrent beds: a laboratory study

Antonino Labate (a.labate@unirc.it)
Department AGRARIA, University “Mediterranea”, Reggio Calabria, Italy
Tutor: Prof. Paolo Porto

Effetti delle opere trasversali di sistemazione sulla evoluzione di alvei sabbiosi: uno studio di laboratorio

ABSTRACT

The role of large engineering control works, such as dam construction and river channel adjustments, is well recognized in many areas of the world. Their downstream impacts on river dynamics, geomorphic processes, and riparian vegetation changes, have been documented in several contributions. However, interactions between small grade-control structures and erosion and deposition processes are less well known. These small structures play a key role in stabilizing natural rivers through a general reduction of the bed slope upstream. This new longitudinal profile, better known as ‘slope of siltation’ or ‘equilibrium bed slope’, depends on the height and distance between structures and on the particle size of the bed. Consequently, a better understanding of the selective sediment transport related to their construction can be useful in predicting the channel evolution of natural rivers. The contribution reported here is based on an experimental laboratory channel, characterized by a sandy bed, where some small control structures have been placed. The experimental runs are aimed at analyzing the variations in terms of channel evolution and sediment particle size before and after their installation. Experiments were carried out in steady sheet flow conditions, varying the slope of the channel from 0 to 0.02 m/m in each run. The particle size distribution of the bed near the structures has been studied using a digital analysis. The overall results indicate an armour coat formation that depends on the bed slope and on the initial grain size distribution. However, further work is required to extrapolate these preliminary results to a field scale.

RIASSUNTO

Il ruolo delle grandi opere di sistemazione fluviale, quali briglie e risagomature d’alveo, è noto in molte aree del mondo. L’impatto di queste opere a valle sulle dinamiche fluviali, sui processi geomorfologici e sulla composizione della vegetazione riparia, è stato studiato in diversi contributi. Tuttavia, le interazioni tra piccole strutture di correzione ed i processi di erosione/deposizione sono meno noti. Questo tipo di opere svolge un ruolo chiave nella stabilizzazione degli alvei naturali attraverso una riduzione complessiva della pendenza del letto a monte. Il nuovo profilo longitudinale, meglio noto come "pendenza di equilibrio", dipende dall'altezza e dalla distanza tra le strutture, oltre che dalle dimensioni delle particelle che compongono il fondo alveo. Di conseguenza, una migliore comprensione dei meccanismi di trasporto selettivo dei sedimenti legati alla costruzione di piccole opere di correzione può essere utile per prevedere l'evoluzione delle aste fluviali. Questo studio è stato svolto su un canale sperimentale a fondo sabbioso allestito in laboratorio, in cui sono state posizionate alcune opere trasversali. Nel corso delle prove sperimentali, al variare della pendenza, sono state monitorate l’evoluzione del canale e la distribuzione delle particelle sabbiose, prima e dopo l’installazione delle opere. Gli esperimenti sono stati condotti in condizioni di portata costante (moto permanente), con valori della pendenza del canale da 0 a 0,02 m/m in ciascun set di esperimenti. La distribuzione delle dimensioni delle particelle del letto a monte delle opere è stata determinata tramite analisi di immagini. I risultati indicano la formazione di uno strato di armoring che dipende dalla pendenza del letto e dalla distribuzione iniziale delle dimensioni dei grani.

STATE-OF-THE-ART

The knowledge of erosion and sediment transport processes is important to control the evolutionary processes of torrents. As response to these processes, sandy-bed torrents dynamically and continually change their morphology (Termini, 2011), in particular where low-frequency and very intense rainstorms induce high erosion rates and sediment transport, as in the fiumaras of Southern Italy. Moreover, the presence of hydraulic structures (such as check dams) considerably modifies these natural changes, which can propagate at distance (Teraguchi et al., 2011). For example, Grade Control Structures (henceforth GCS), which prevent from excessive channel profile degradation, generally play downstream an erosive action that causes significant bed scouring (with possible risk of structure collapse), which, as broadly emphasized in eminent literature (Lenzi et al., 2003), (Simon et al., 2002), (Termini, 2011), (Termini et al., 2012), must be studied and faced off.

In order to improve the installation and optimize the hydraulic functioning of engineering control works, there is the need of design criteria for structures controlling the hydro-geological instability and disruption in torrents of the Mediterranean zones. The current methods to quantitatively predict the morphological response of Mediterranean torrents to GCS presence are often time-consuming and require specialized knowledge for suitable applications. This makes them impractical to be used by planners and thus torrent response is either ignored or determined by inappropriate methods.

Vice versa, laboratory investigations, aiming at simulating at small scale the erosion and sediment transport processes and their interactions with engineering structures, may suggest more suitable models of morphological evolution of torrents with GCS.

The use of laboratory flumes to explore water and sediment flow is a common practice, as confirmed by many experiences reported in literature: as an example, Curran and Wilcock (2005) conducted experiments in a small flume to examine the characteristic dimensions of the step-pool bed configuration; Hancock and Willgoose (2004) studied the effects of erosion on a tailing check dam under simulated rainfall; Chen and Hong (2001) analyzed the characteristics of check dam scour hole by free over-fall flow; and Xu et al (2006) simulated runoff and erosion/deposition processes in a channel with a check dam.

INTRODUCTION

Main goal

The aim of this Ph.D. thesis is to evaluate, on an experimental basis, the effects of torrent Grade Control Structures on channel erosion/deposition processes over time and space. To this goal, the evolutionary processes of an artificially graded sandy-bed torrent were simulated at laboratory scale; from these experiments, design criteria for sizing transversal control works will be proposed.

Premise

Sediment transport is a significant component of many environmental degradation problems. The process of sediment transport understanding, however, is complicated by the interaction of many parameters, including particle size of the river bed. In fact because river beds are mainly composed by non uniform materials, if flow conditions are such that sediments of every size are not in motion, a protective layer, known as the armor layer, develops on the bed surface (Image 1). With the formation of an armor layer, further erosion of the bed is stopped, but finer sediment particles from upstream may move downstream over the armor layer.

The armoring process is important in river engineering studies, for example, in the study of river bed degradation/aggradation near engineering control works due to the imbalance of sediment that is created near the structures.

When the threshold of movement for a particle in a river bed is exceeded, it starts to moves. In a sediment mixture, the resistance to movement of individual particles depend on the particle size, shape, and density, as well as covering and exposure to the flow. Typically, finer or exposed particles tend to move first, starting the development of clusters of particles on the surface, with larger, more stable particles. This is a dynamic phenomenon: the clusters continually break and new ones forms. The particle rate of removal from the surface decreases with time tending to zero, as an asymptotic process. At any applied fluid shear stress the bed surface approaches to a dynamic armor condition. If the shear stress on this armor is reduced, the dynamic armor becomes a static one, when all particles have a higher threshold to movement of that exerted by the reduced flow and the transport of sediment from upstream may still occur over a static armor. If the bed shear stress on an equilibrium dynamic armor is increased, more of the particles of the surface layer are set in motion and a new process of surface armoring starts. At the end, a limiting condition is reached, called critical armoring condition. At higher shear stresses all particles are put in motion and no armor develops. The limiting shear stress is called

the critical shear stress. Hence a mixture has a range of bed shear stresses over which its bed surface can armor. The range of armors depends on the parent bed material. Considering nonuniform sediments with the same specific gravity for all particle sizes, a bed material with a wider range of particle sizes especially among the coarsest fractions, tends to have a wider range of possible armor layers than that of a bed material with a shorter range of particle sizes.

Several researchers, including Gessler (1967), Little and Mayer (1972, 1976), Proffitt (1980), and Sutherland (1987) have presented laboratory data on armoring. Most of the experiments were limited in sediment size range and were conducted at relatively low shear stresses.

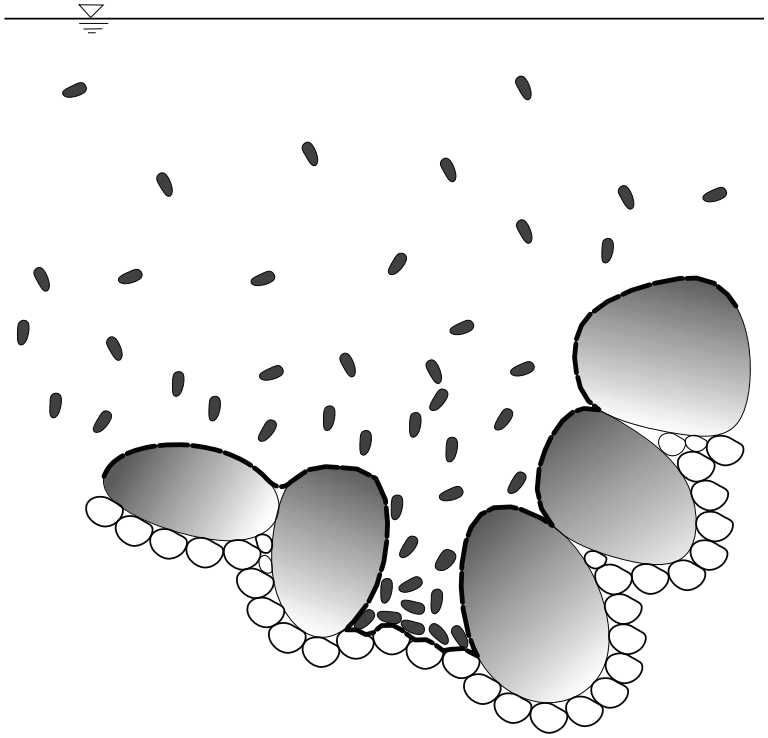

Image 1: Mixing layer in dinamic armoring process (redrawn from Di Silvio and Brunelli, 1989)

Various approaches in the investigation of sediment motion problems in rivers and channels have been used and they have been adopted for the assessment and analysis of particular problems associated with sediment transport. One aspect of sediment motion that is an important component of many engineering studies is the incipient motion of particles. This identifies the moment at which particle motion begins and it is dependent on the particle size, particle shape, specific weight of particle and flow conditions. Once motion begins, sediment particles may slide or roll on the bed (bed load), or be carried along in suspension by the water (suspended load). In order to understand the transportation of sediment in a channel, it is necessary to be able to define the critical shear stress, which is defined as the smallest shear stress necessary to move a sediment particle. The threshold of particle motion is defined as the condition for which the applied forces just exceed the resistance force; at critical shear stress, the condition is defined as incipient motion, or the point of which sediment particles are ready to move but are not yet moving.

The critical force required to initiate the motion of sediment particles has been associated mostly with two general theories. The first one, which was presented by Hjulstrom (1935), is based on the cross-section mean velocity of the flow required for the transport of a certain particle size. The plot proposed by the author (Image 2) shows the relationship between the size of sediment and the velocity required to erode, transport it and deposit it. The critical erosion curve shows the minimum velocity required to lift a particle of a given size, while the critical deposition curve shows the maximum velocity at which a river can be flowing before a particle of a certain size is deposited. The zone in-between is the zone of transport.

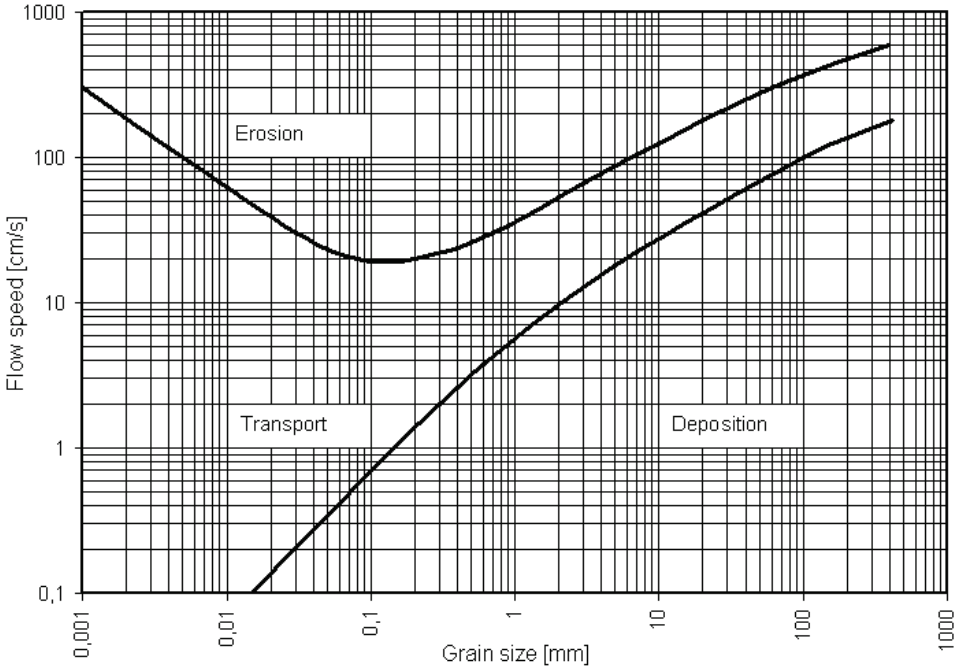

Image 2: Hjulstrom diagram (1935)

The second theory is based on the time averaged critical shear stress (τ_c) and was developed from the early 19th century by Du Buat (1816), Du Boys (1879), Schoklisch (1932) and Shields (1936). Shields considered the force acting on sediment as a shear force, assuming that the resistance of the particle to motion depends only on the shape of the bed and the submerged weight of the particles. He studied these forces for different flow conditions and showed that the threshold of particles movement could be represented by a non-dimensional relationship for a uniform sediment in unidirectional, uniform flow, on the basis of the relation between shear stress and the grain Reynolds number, given by the following formulas:

$$\tau^* = \theta_c = \frac{\tau_0}{(\rho_s - \rho_w) \cdot g \cdot d} \quad (1)$$

where τ is the shear stress, ρ_s and ρ_w the density of sediment and water, respectively, g is the acceleration of gravity, d is the considered particle diameter

$$\mathrm{Re}^* = \frac{\mu \cdot D}{\nu}$$

with μ shear velocity, D particle diameter, ν water kinematic viscosity.

These values are plotted on the Shields diagram, which discriminates zones with or without sediment motion (Image 3). Shields determined the critical shear stress of particles by plotting the observed sediment flux versus shear stress and Equation 1 was obtained from a dimensional analysis verified by experimental data. After Shields, some investigators (White, 1940; Egiazaroff, 1957; Lane, 1955) derived some relationships for the initiation of motion.

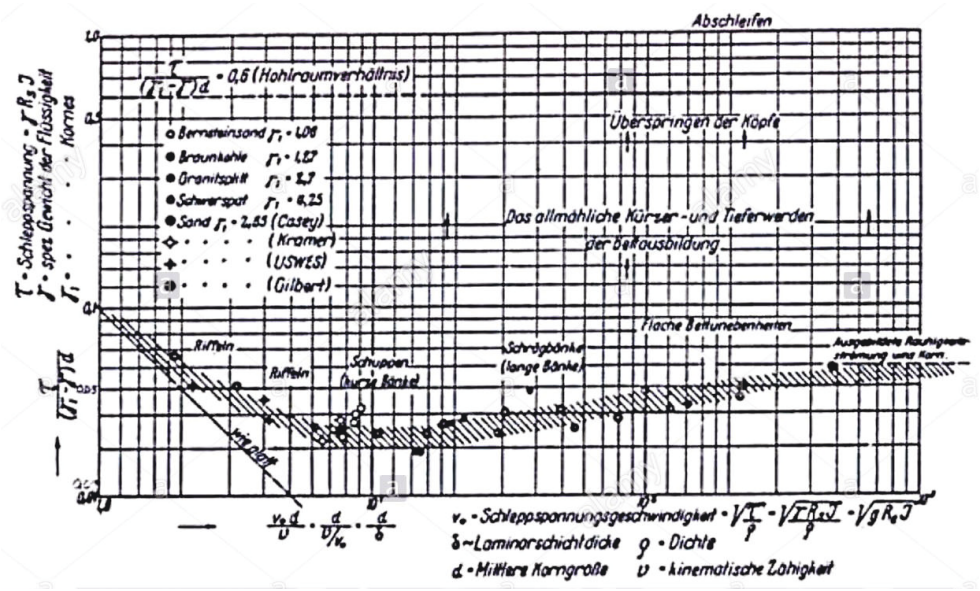

Image 3: Shields diagram, from Shields (1936)

Lane's relation

This qualitative relation was introduced by Lane (1955), stating that water discharge (Q_w), channel slope (S), sediment discharge (Q_s), and a representative bed sediment size (D_s) in a river under equilibrium conditions are linked in the form:

$$Q_s \cdot S \propto Q_w \cdot D_s \quad (2)$$

This relation (Image 4) provided for long time a conceptual model used in various field (Julien, 2002; Dust & Wohl, 2012): a change in any of the four variables will cause a change in the others until the equilibrium is restored. When a channel is in equilibrium, it will have adjusted these four variables such that the sediment being transported into the reach is transported out, without significant deposition of sediment in the bed (aggradation), or excessive bed scour (degradation).The Lane's conceptual relationship fits the concept of dynamic equilibrium established by Schumm (1977) and is, therefore, applicable to most streams and rivers. A limitation of this conceptual model is that it does not indicate which variable will adjust, the magnitude of the adjustment, or the timeframe that will be involved.

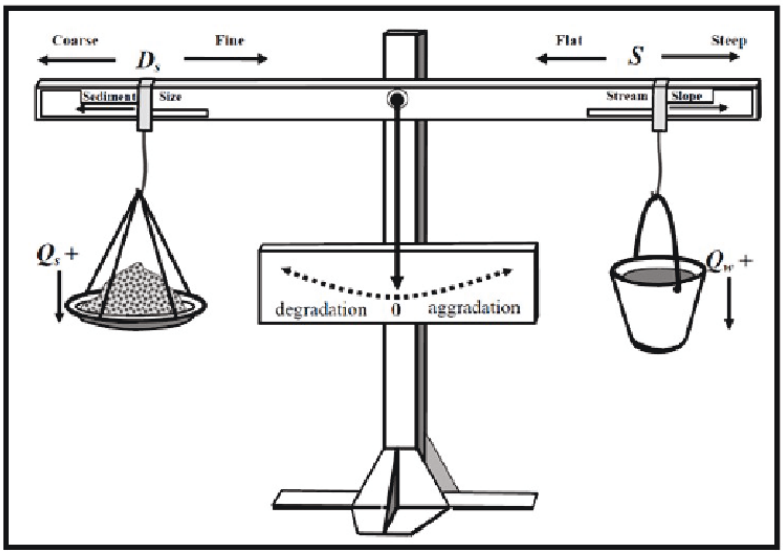

Image 4: Lane's balance (from Wohl et al., 2016)

Sediment classes and gradation curve

In natural rivers, the bed material is made of non-uniform mixture of particles. During the flow events the continuous sediment exchange between bed surface and transported load, as well as channel aggradation/degradation processes, modify in time and space the composition of both the transported and bed materials (Einstein, 1950).

The sediment carrying capacity also is closely related to the grain size distribution, which has direct impact on the erosion and deposition on the river bed so, how to predict bed sediment composition is essential for successfully applying numerical models to simulate sediment transport and river dynamics. Generally, the bed material dimensional characteristics are described by dividing the sediment mixtures into several fractional groups and providing their corresponding proportions. A first approximation useful to describe the soil and/or the sediment dimensional composition, is the determination of the sample texture, an important parameter used to evaluate some physical properties (Saxton & Rawls, 2006) and it is defined classifying the relative percentage of soil separate (clay, silt, sand) using one of the available soil texture classification methods. One of the most used methods worldwide is the one from the USDA (2017), where the soil is identified using eight major classes, ranging from *'clay'* to *'gravel'* (Image 5).

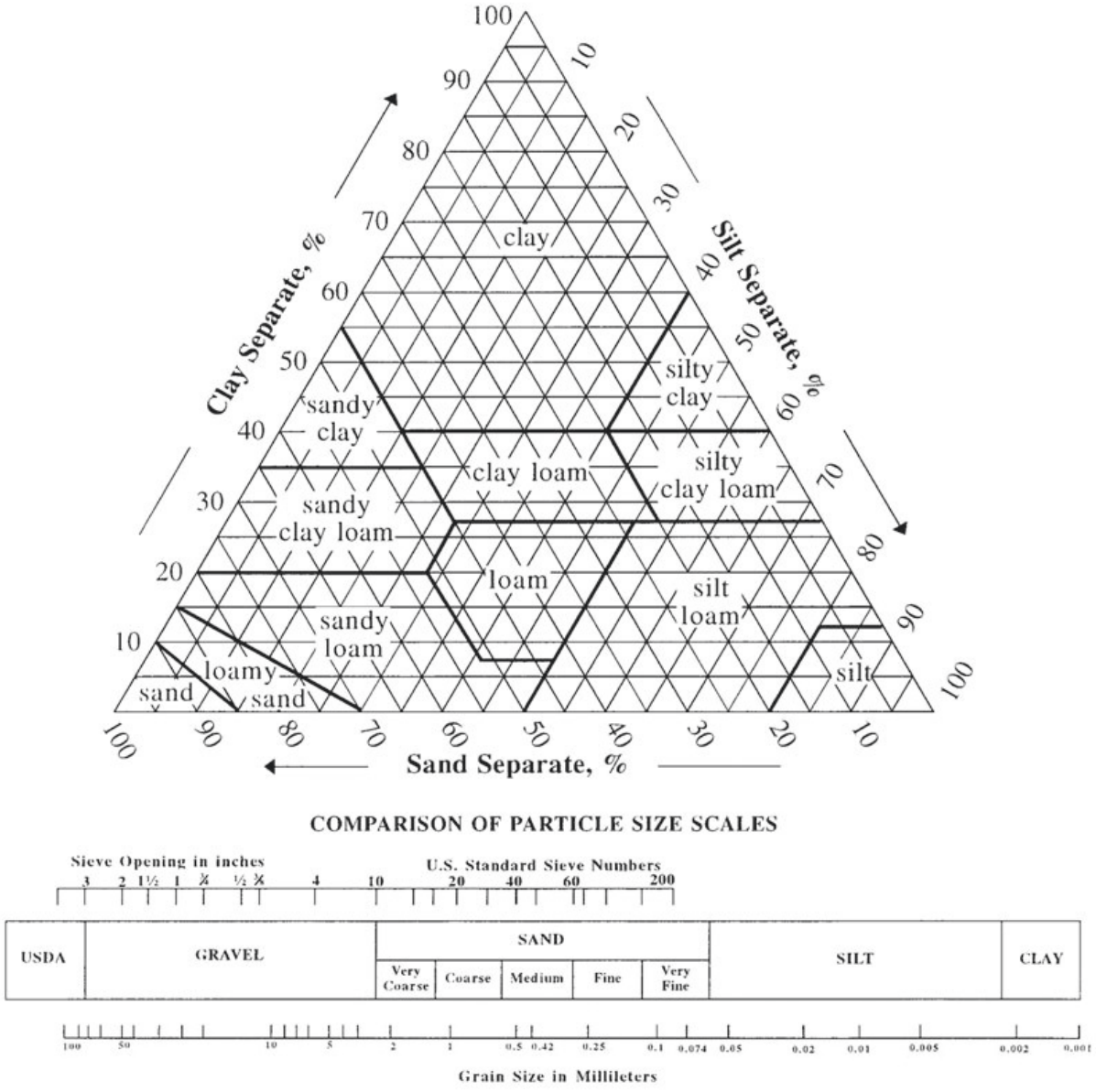

Image 5: Soil texture triangle, showing the major textural classes, and particle size scales as defined by the USDA (1987)

The most common way to represent the soil particle size distribution is using a “gradation curve”. This is a representation on the Cartesian axes where the soil particle diameters is on the x-axis and the cumulative frequency (on a 100% basis) is on the y-axis. There are several methods to calculate the relative frequency of each class, and the most widely used are:

- Sieve analysis (Krumbein & Pettijohn, 1938; ISO, 2000): the soil sample is placed on the top of a mechanical shaker tower, composed of sieves with different mesh opening. After some time from the start of the shake, the sample retained from each sieve is weighted and compared to the sample total weight using the formula:

  $$\% \text{ retained} = W_i / \Sigma W_i \quad (3)$$

  $$\% \text{ cumulative passing} = 1 - \% \text{ cumulative retained} \quad (4)$$

  where W_i is the weight retained in the i-esim sieve and ΣW_i is the total weight of the aggregate.

- Optical particle measurement (Agrawal *et al.*, 1991; Walling and Collins, 2010): this kind of analysis, can be performed by different types of equipment. Here, as an example, the procedure based on the use of an *Analysette 22* laser particle sizer is described because it was applied in this thesis. The analysis consists of a series of steps:
  1. the organic matter in the soil sample is oxidized using Hydrogen peroxide (H_2O_2) until there is no production of gas;
  2. the resulting sample is mixed with a chemical dispersal (sodium hexa-meta-phospate $(NaPO_3)_6$), centrifuged for two hours at 2000 r.p.m. and divided from the supernatant fraction;
  3. the sample goes then in the laser particle sizer, where any eventual aggregate is further disrupted with high frequency sounds and the size of each particle is determined by refraction of laser light (Image 6).

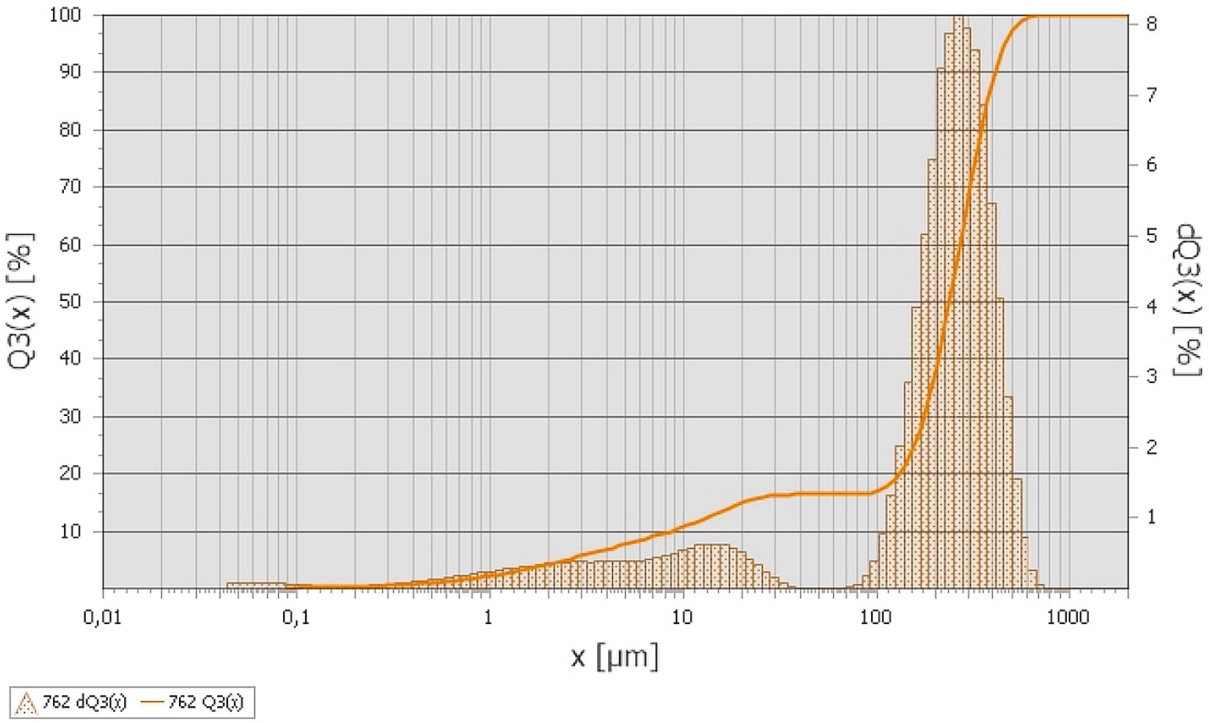

Image 6: Soil sample particle distribution

- Digital image processing (Sid-Ahmed, 1995; Mora *et al.*, 1998; Schneider *et al.*, 2012): this methodology includes two steps: the first phase is the spatial calibration of the image, needed to convert the length from pixel units to real spatial units: this is usually done measuring an object with known length and calculating the pixels/mm proportion to apply later. In the second part, the length of both long and short axis of every sand grain is recorded and each measurement is automatically converted in spatial units (mm). This method has the advantage to leave the channel bed untouched and it has become of more common use from the 90s of the last century, having high resolution images available.

MATERIALS AND METHODS

EXPERIMENTAL SETUP

The Flumes

The experimental activities were carried out at laboratory scale using two experimental flumes. The first was the one available at the "Agricultural Hydraulics and Watershed Management" laboratory of the "Mediterranea" University of Reggio Calabria (Italy).

The flume consists of a 1.60-m plastic channel with rectangular section (0.08 m x 0.115 m). Water flow, recirculating by a pump, is fed from an upstream stilling reservoir with a maximum depth of 0.195 m. A rectangular weir, placed downstream of the flume, allows the measurement of the water discharge. No sediment feeding system was adopted. The main hydraulic (e.g. water discharge), geometric (e.g. longitudinal slope and check dam size) and bed (e.g. sediment grain size) parameters of the experimental flume can be easily setup and controlled. The layout of the experimental flume is shown (Image 7).

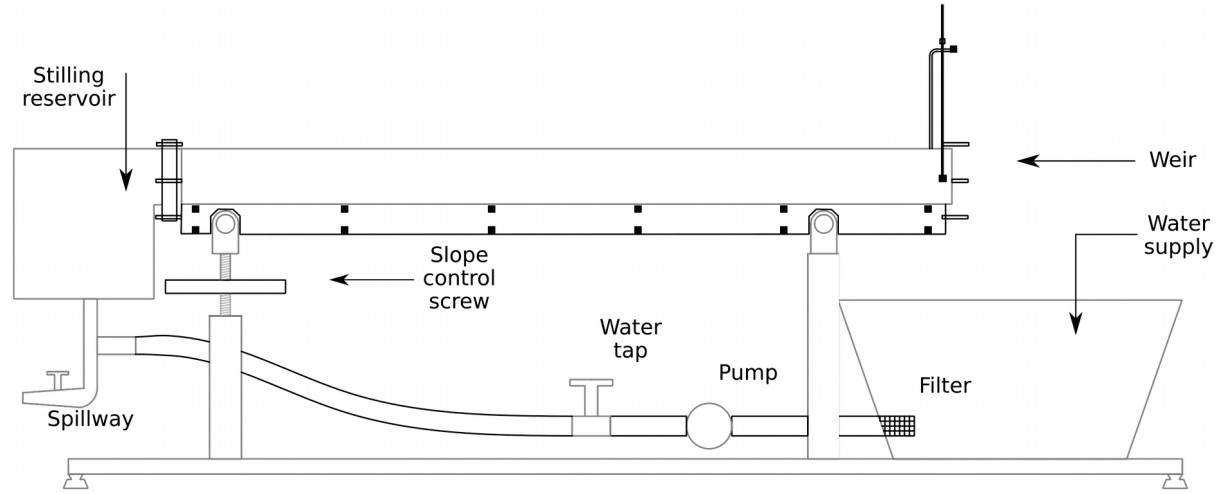

Image 7: Experimental flume used for the experiments

Water discharge took the constant value of 0.33 l/s, and this value was calculated from the water head measured with point gauge in correspondence of the weir. In each experiment, sediment was then mixed by hand and leveled up flat to the height of the GCSs (4 cm), over all the length of the flume. The channel bed slope was the variable parameter during all experiments. A control region, placed halfway along the channel, was used as a reference to acquire the images of the studied area, upstream of each of the GCS (Image 9).

The experiment set was expanded making use of a bigger laboratory flume (Image 8) during a period abroad, at the Warsaw University of Life Sciences SGGW (Szkoła Główna Gospodarstwa Wiejskiego) also used to verify the extensibility of the experimental results to different scale. The channel used at the Hydraulics laboratory of the Faculty of Civil and Environmental Engineering was 0.58 m wide and 10.00 m long. A solid bottom, (5.82 m in length), precedes the 2.18 m long washout part, filled with sand (median grain diameter d_{50} = 0.62 mm, d_{90} = 1.50 mm). A pin water gauge was used in order to measure the water surface elevation, regulated with a gate. The level of the sandy bottom within the washout bed was measured through the transparent side wall. The water flow discharge was set using an electromagnetic flow meter. No sediment feeding system was adopted. However, since the results obtained with the second channel are preliminary, they were not included in this study.

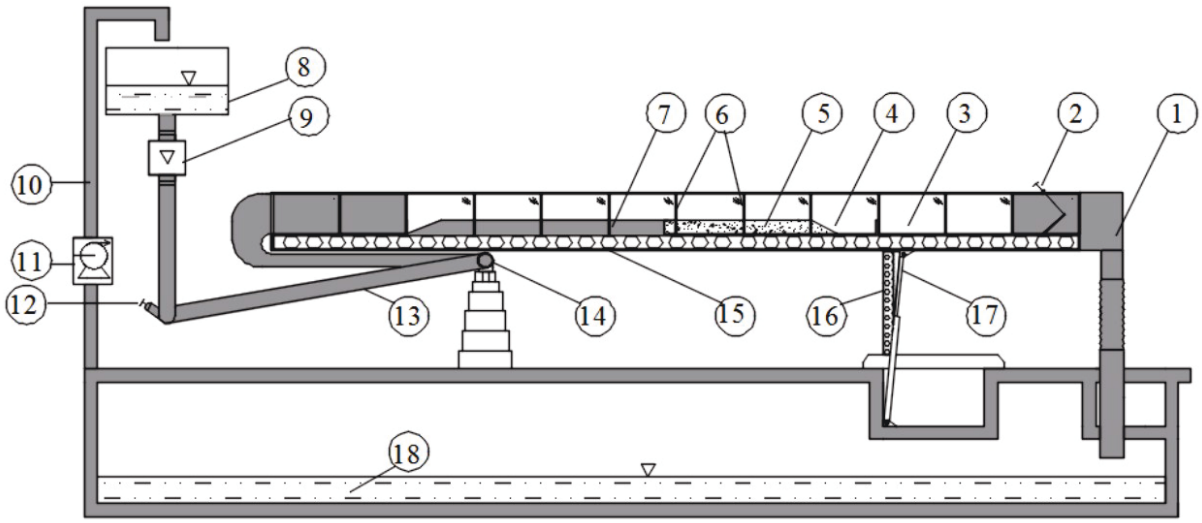

Image 8: Experimental channel scheme, side view (From Kiraga and Popek, 2016). 1 chute chamber; 2 regulatory gate; 3 glass side wall; 4 collection chamber; 5 sandy bed; 6 supports for side walls; 7 solid bottom; 8 upper reservoir; 9 electromagnetic flow meter; 10 pipeline conducting water; 11 pump; 12 regulatory valve; 13 feeding pipeline; 14 support with joint; 15 support plate of the channel; 16 support with adjustable frame elevation; 17 hydraulic cylinder; 18 lower reservoir.

As pointed up by Koll (2004) the transport rate of bed material was higher at the beginning of the experiments, getting lower over the duration of the run: the time needed to reach equilibrium for each experiment was of about 3-4 hours.

Bed material characteristics

The sediment used in the experiments was desalinized sea sand (Bulk density = 1320 $kg \cdot m^{-3}$) with size ranging from 0.2 to 2.0 mm (USDA upper boundary for sand) and the upper limit was imposed by sieving the sediment to avoid the presence of gravel or cobbles. Organic matter was disrupted using hydrogen peroxide (H_2O_2) to completely oxidize it.

Analysis of the sand diameters

The ImageJ software was used to measure the diameters of the sand grains. ImageJ is a Java based image processing program developed from the U.S. National Institutes of Health and the Laboratory for Optical and Computational Instrumentation (LOCI, University of Wisconsin), designed with an open architecture that provides extensibility via Java plugins and macros. It was born for biomedical microscope images analysis, but is commonly used in various different fields of research such as astronomy, archaeology, hydraulics, ecc.

Dimensions in a digital image are measured in number of pixels, so the first required step is to calibrate the image to obtain lengths in real spatial units. After this it was possible to perform an image-based grain-size analysis, measuring the length of both long and short axis of every sand grain (Image 9c). Measurements, in steady flow conditions, were made both before and after the placement of the GCS comparing, at the same bed slope, the grain diameters corresponding to percentiles.

This kind of measurement mimics the “grid-by-number” method (Wolman, 1954), based upon an analysis of the relative area covered by particles of different sizes; the method is usually applied to rivers with coarse bed material. From the sampled measurements a frequency distribution is drawn. The acknowledged advantages of this sampling procedure over bulk sampling are the applicability to very coarse materials, and that it provides a more representative sample of an entire reach of a stream. This measurement technique (Schneider et al., 2012) gives very accurate results: during the calibration step a standard deviation σ of 0,04 mm (standard error of the mean = 0,0028) was reached.

The obtained measurements were then processed obtaining, as a result, the grain-size distribution of the sediments. Characteristics diameters of the mixture were as well calculated and, given the non-normality of the empirical grain diameters distributions, the two-sided Kolmogorov-Smirnov test (or K-S test) was used to evaluate the presence of statistically significant differences between distributions. This non-parametric test quantifies the distance between the empirical distribution functions of two samples, under the null hypothesis that the samples are drawn from the same distribution. The advantage of the two-sample K-S test on other non-

parametric methods for comparing two samples, is the sensitiveness to differences in both location and shape of the empirical cumulative distribution of the two samples.

To efficiently perform the required calculations on the grain-size measurements, some script in Python were developed, aimed to plot frequency distribution curves, to calculate distributions univariate statistics and to perform statistical significance tests (Appendix A).

Python is an open-source, interpreted, high-level and general-purpose programming language created by Guido van Rossum in 1991, with a design philosophy that emphasizes code readability, using significant whitespace and code indentation. It provides constructs that enable clear programming on both small and large scales. Python features a dynamic type system and automatic memory management. It supports multiple programming paradigms, including object-oriented, imperative, functional and procedural, and has a large and comprehensive standard library.

In addition to the standard library, there is a growing collection of several thousand components, available from the Python Package Index. In particular during this work NumPy, SciPy and Pandas libraries were used to perform calculations and organize data, while Matplotlib and Seaborn libraries were used to produce plots and graphical objects.

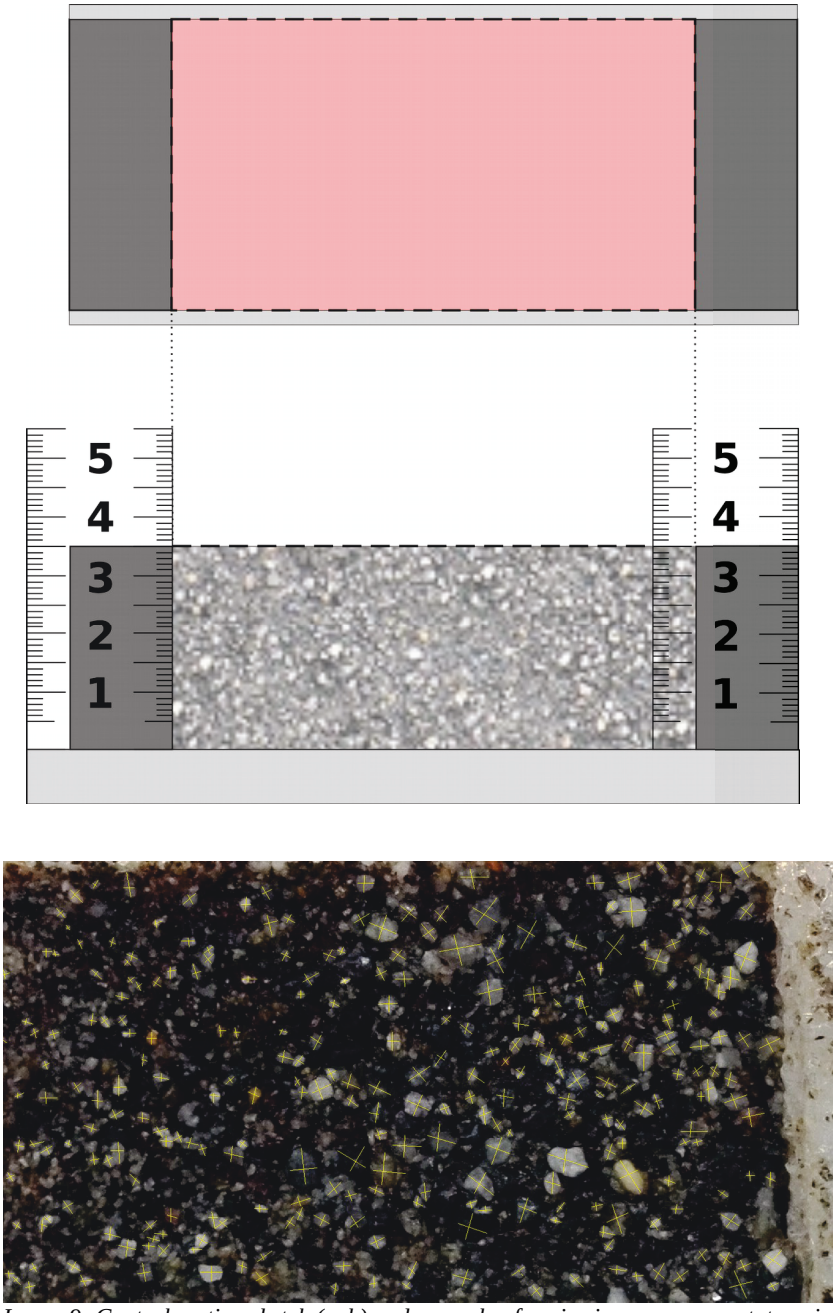

Image 9: Control section sketch (a, b) and example of grain size measurement, top view (c)

Channel bed configurations

The experimental activity involved the use of multiple channel configurations, aimed to analyze different conditions of longitudinal slope, and different contexts of channel correction: the experiments were conducted both in conditions of simple sandy bottom and in the presence of one or three GGS, in order to simulate the effects of isolated structures or articulated in a system, assessing the effects of these configurations on the grain size assortment.

No Grade Control Structures

The first set of measurement was acquired in the absence of GCS, in order to investigate the evolution of the channel at different bed slopes. A movable sandy bottom was made (see "bed material characteristics" paragraph above) with a height equal to that of the GCS used in subsequent experiments (4 cm). The experiments were carried out in steady flow condition and bed image were taken before the start of the runoff and after an adequate stabilization time from the start of each run. Every run required an interval of about 4 hours to reach transport equilibrium.

Single Grade Control Structure

The second configuration was prepared using a single polyethylene GCS located in the middle of the control area. The GCS had a height of 4 cm and was placed in the middle of the channel, to avoid being influenced by the turbulence coming from the beginning of the channel and by the (backwater effects?) due to the weir placed at the end of the flume. The experiment took place in the same way as in the previous set.

Three GCS configuration

This experimental configuration used was a three-object design, with three GCS (height = 4.0 cm, thickness = 1.5 cm), with a height:distance ratio of 1.5 (d = 6 cm) and 3 (d = 12 cm): these ratios are commonly used in the first-approximation design of Grade Control Structures. Also in this case the GCS were placed in the middle of the channel, varying only the bed slope for each simulation.

UP-SCALING AND SIMILITUDES

Geometric, dynamic and kinematic similitudes

The aim of these laboratory experiments is to evaluate the effects of GCS on the channel dynamics and, as the size of the flume is different from that of a real river, to correctly represent the processes, it must respect the constraints imposed by the laws of similitude.

The use of small-scale prototypes that represent real phenomena is a well-established practice in the hydraulic field for over a century of experimentation (Reynolds, 1888; Gilbert, 1914), providing numerous advantages compared to full field experimentation (Table 1), such as exact knowledge of the initial conditions, need for less quantities of materials, lower realization costs, the possibility of functioning in a wide range of boundary conditions. The fundamental assumption for this type of scale model to represent a phenomenon correctly is to take into account the Similitude laws (geometric, dynamic and kinematic similarity):

Geometric similarity (similarity of shape): Where boundaries of solid bodies are considered, the characteristic property of geometric similarity is that the ratio of any length in one system to the corresponding length in the other system is the same throughout; this ratio is usually called scale factor $\lambda = L_p \cdot L_m^{-1}$; (where 'p' denote the prototype and 'm' the model). Consequences of respected geometric similarity are: $Area_p = \lambda^2 \cdot Area_m$; $Volume_p = \lambda^3 \cdot Volume_m = \lambda^3 \cdot mass_m$, (if $\rho_p = \rho_m$)

Kinematic similarity (similarity of motion): When the flow in a model is geometrically similar to that in the prototype, then these two systems are said to possess kinematic similarity. However, solid boundaries themselves are streamlines, so geometric similarity of models is a prerequisite. Similarity of motion also implies similarity of time intervals. Being the corresponding lengths and time intervals in two systems in a fixed ratio, the corresponding velocities (and accelerations) must be as well in a fixed ratio at corresponding times.

Dynamic similarity (similarity of forces): It exists when the ratio of corresponding forces is constant. The forces that may be relevant include inertial, gravitational, viscous, elastic, pressure, capillary

It is possible to demonstrate that the more the scale ratio deviates from 1:1, the more difficult it becomes to preserve the integral similarity of the model (Yalin, 1971), therefore it is common practice to preserve the similitude for the most representative aspects of the phenomenon investigated in the model, accepting a distortion in the other cases: in particular, the similarity of Reynolds is preserved to respect the ratio of inertial to viscous forces, while the Froude similarity to preserve the ratio of inertial and gravitational forces.

Dimensionless quantities

For a consistent description of physical processes, is required that all terms in an equation have the same units. On the basis of physical laws, some quantities are dependent on other quantities. The Buckingham π-theorem provides a basis for all non dimensionalization. In fluid mechanics, Navier-Stokes equation, a partial differential equation, describes the flow of incompressible fluids.

The full set of Navier-Stokes equations is very complex and it is often more useful to search for approximations valid for certain specific circumstances, instead of looking for the general solutions. To make systematic approximations it is necessary to have a procedure that helps us discern precisely what is significant and what is not. A standard procedure is to first find the scales relevant to the problem. Normalization by these scales leads to dimensionless parameters which represent the relative importance of various parts of the full equations.

Dimensional analysis indicates that the dominant forces in a free surface flow are mainly inertial, gravitational and frictional, so the conversion from model to prototype quantities have to satisfy the Froude number similarity, that is $Fr_m = Fr_p = (U^2 / g\ L)^{0.5}$, where U is the mean flow velocity, g is the constant of gravity acceleration and L is a typical dimension of the model.

Table 1: Summary of studies employing movable-bed physical models (From El Kadi Abderrezzak et al., 2014)

Reference	Scaling criteria		Model characteristics	Phenomena investigated	Model-prototype comparison
	Satisfied	Relaxed/ignored			
Song and Yang (1979)	$V \times S/w_s$	F, d/h, θ, θ_c, Re_*	Distorted. Uniform sand. Froude number exaggerated by a factor of 1.9	Maintaining of navigation conditions at a river confluence	Yes
Parent (1988)	F, θ, θ_c	d/h, Re_*	Undistorted. Non-uniform sand mixture (truncated to avoid ripple formation)	Morphology and sedimentology of pool-riffle sequences	Yes
Young and Warburton (1996)	F, θ, d/h	θ_c, Re_*	Undistorted. Natural material. Flow is rough turbulent in the model	Morphology and sedimentology in braided gravel-bed rivers	Yes
Healey (1997)	F, θ	d/h, θ_c, Re_*	Undistorted. Mix of sand and gravel. Bank failure not reproduced	Evaluation of methods for the mitigation of embankment (bank) erosion	Yes
Davinroy et al. (1999), Gaines and Maynord (2001), Rodgers et al. (2003), Maynord (2006)		F, d/h, θ, θ_c, Re_*	Distorted. Lightweight particle (plastic)	Design of channel-control alternatives (dikes, bendway weirs, bank line changes)	Yes
Wallerstein et al. (2001)	F	d/h, θ, θ_c, Re_*	Distorted. Uniform sand (one grain size)	Geomorphic and hydraulic impact of large woody debris	No
Wei et al. (2001)	F, θ/θ_c, $B \times S/h$	d/h, θ, θ_c, Re_*	Distorted and undistorted models are tested. Uniform sand and lightweight particles (Lapili) are tested	Evaluation of bed load and bar formation following training works	No
Woidt et al. (2001)	F, θ/θ_c	d/h, Re_*	Undistorted. Cohesive loam soil for the bank. Fine silica sand for the bed	Sedimentation at a pump intake	No
Waldron (2005)	F, θ, θ_c, Re_*	d/h	Distorted. Lightweight particles (synthetic plastics), uniform size	Efficiency of sediment diversions for rehabilitating degraded wetlands	No
Marr et al. (2007)	F, θ	d/h, Re_*, θ_c	Distorted. Mix of coarse and fine sand	Rate and timing of remobilisation of stored sediments following dam removal	No
Bennett et al. (2008)	F	d/h, θ, θ_c, Re_*	Distorted. Sand, uniform particle size	Use of in-stream woody vegetation for restoring meandering pattern	No
Bromley (2008)	F, θ	Re_*, θ_c	Distorted. Mix of sand and gravel. Supercritical flow	Downstream morphology changes due to dam removal	Yes
Mefford et al. (2008)	F, $(\theta - \theta_c)$	d/h, θ, θ_c, Re_*	Undistorted. Mix of sand and gravel. Silt and clay material are not represented in the model	Performance of a high-flow bypass spillway in improving bed load transport at a diversion dam structure	No
Pugh (2008)	F, $q_s/(u_* d)$, w_s	d/h, Re_*, θ, θ_c	Distorted. Uniform sand	Design of channel-control alternatives for limiting sediment intake at a planned diversion dam	No
Weitbrecht and Rüther (2009)	F, θ_c	d/h, θ, Re_*	Undistorted. Mix of sand and gravel. Finer fractions of the model sediments are coarsened, fractions of grain sizes <0.2 mm are eliminated	Performance of a planned drift wood retention concept in an expanding river reach	No
Armanini et al. (2010)	F, θ, θ_c	d/h, Re_*	Undistorted. Lightweight particles (plastics), uniform particle size. Finer fractions are not reproduced	Design of groynes to improve navigation condition	No
Ho et al. (2010)	θ, θ_c, Re_*	d/h, F	Distorted. Lightweight particles (crushed coal). Uniform particle size. Subcritical flow ($F < 0.5$)	Sediment exclusion at an intake structure	No
Mefford and Gill (2010)	F, $q_s/(u_* d)$, w_s	d/h, θ, θ_c, Re_*	Distorted. Lightweight particles (coal), uniform size	Evaluation of different restoration works for creating shallow water habitat along a stream bend diversion	No
Simonett and Weitbrecht (2011)	F, θ/θ_c	d/h, θ, θ_c, Re_*	Undistorted. Transcritical flow. Mix of sand and gravel. Finer fractions are coarsened, fractions of grain sizes <0.2 mm are eliminated	Design and optimisation of training works for flood defence	No
Bieri et al. (2012)	F	d/h, θ, θ_c, Re_*	Undistorted. Non-uniform sand mixture	Design and optimisation process for sediment flushing operation	Yes

RESULTS AND DISCUSSION

As is well known, (Gessler 1971, 1990) the presence of an armor layer increases the resistance to the bed surface disruption. The increase of finer particles at lower slope values could probably be due to a kinematic sorting effect (Wilcock, 2001) for which smaller particles clusters in the empty spaces between coarser grains, gaining stability towards flow, and slowly going down in the subsurface layers, according to the scheme of Di Silvio & Brunelli (1989).

Considering that the main aim of this kind of structures is to prevent excessive channel profile degradation, the selection of larger grains at higher bed slope values is a further contribution to maintenance of the wanted longitudinal shape, being more energy required for the erosion of such sediments. At the same time, finer grains can travel through the channel up to the sea, contributing to the mitigation of coastal erosion.

Effects in clear water

In a first phase the experimental flume was characterized from the hydraulic point of view, inferring roughness coefficient of the channel (plexiglass) and defining the possible velocity/flow dominion based on the pump characteristic and the channel geometry. Dimensionless group usually used in fluidodynamics were also evaluated:

- the Froude number (Fr) is a dimensionless number defined as the ratio of the flow inertia to the gravity and it is based on the speed–length ratio which he defined as:

$$Fr = \frac{u_0}{\sqrt{g_0 l_0}} \tag{5}$$

where u_0 is the characteristic flow velocity, g_0 is in general a characteristic external field, and l_0 is a characteristic length.

- the Reynolds number (Re) is another dimensionless quantity used in fluid mechanics to predict flow behavior in different flow situations and in scaling of fluid dynamics problems, it is the ratio of inertial forces to viscous forces within a fluid which is subject to relative internal movement due to different fluid velocities: this relative movement generates fluid friction, which is a factor in developing turbulent flow. This effect is counteracted by the viscosity of the fluid, which inhibits turbulence, being more kinetic energy absorbed by a more viscous fluid. The Reynolds number quantifies the relative importance of these two types of forces for given flow conditions and it is able to predict the transition from laminar to turbulent flow: laminar flow occurs at low Reynolds numbers, where viscous forces are dominant (smooth, constant fluid movement); conversely, turbulent flow occurs at high Reynolds numbers and is dominated by inertial forces, which tend to produce vortices and other flow instabilities. The Reynolds number is defined as:

$$\mathrm{Re} = \frac{\rho u L}{\mu} = \frac{u L}{\nu} \tag{6}$$

where:

ρ is the density of the fluid (SI units: $kg \cdot m^{-3}$);

u is the velocity of the fluid with respect to the object ($m \cdot s^{-1}$);

L is a characteristic linear dimension (m);

μ is the dynamic viscosity of the fluid ($N \cdot s \cdot m^{-2}$ or $kg \cdot m^{-1} \cdot s^{-1}$);

ν is the kinematic viscosity of the fluid ($m^2 \cdot s^{-1}$).

This information allows to hydraulically define the stream characteristics. The interpolation of measurement of water stage h and corresponding flow $Q(h)$, respectively measured with the volumetric method and the thin-edged (Bazin) weir formula (mean discharge coefficient μ equal to 0.635), led to the identification, in conditions of steady flow, to the stage-discharge curve in the well known power equation $Q = \alpha h^{\beta}$ (Ackers et al., 1978).

The coefficients derived from the experimental data (Image 10) are $\alpha = 61.241$ e $\beta = 1.284$ ($r^2 = 0.984$).

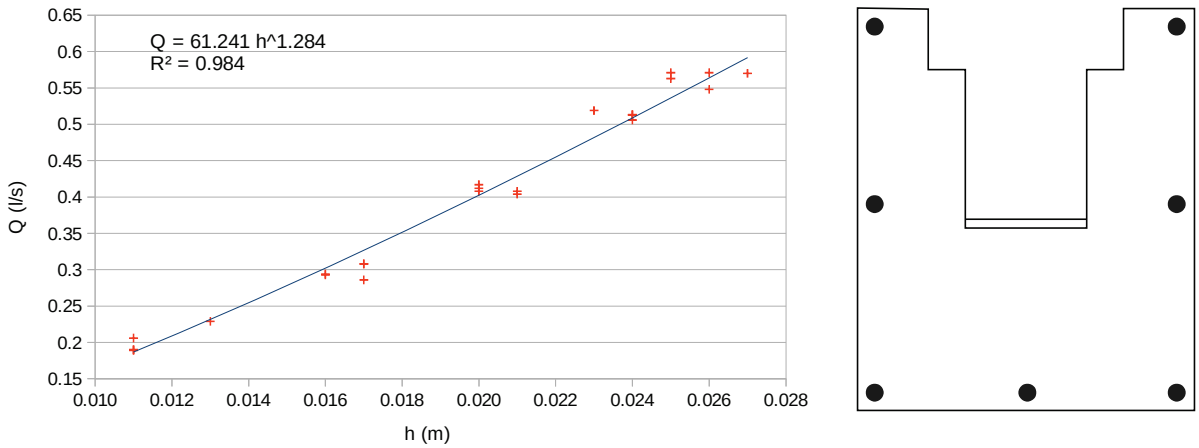

Image 10: Stage-discharge curve for the experimental flume and sketch of the weir.

The other main hydraulic parameters, related to the hydraulic head, are reported in Table 2:

Table 2: Experimental flume hydraulic parameters, horizontal bed.

h *[m]*	**R** *[m]*	**tau** *N m^{-2}*	**Tau* = theta** *[-]*	**u*** *[m s^{-1}]*	**tau_c** *[N m^{-2}]*	**Re** *[-]*	**u** *[m s^{-1}]*	**Q** *[l s^{-1}]*	**q** *[m^3 sm^{-1}]*
0.005	0.004	0.262	0.040	0.016	0.262	6.437	0.209	0.068	0.001
0.010	0.008	0.471	0.073	0.022	0.262	8.637	0.310	0.163	0.003
0.015	0.011	0.642	0.099	0.025	0.262	10.086	0.381	0.277	0.006
0.020	0.013	0.785	0.121	0.028	0.262	11.150	0.436	0.411	0.009
0.025	0.015	0.906	0.140	0.030	0.262	11.977	0.479	0.557	0.012
0.030	0.017	1.009	0.156	0.032	0.262	12.643	0.515	0.677	0.015

h: water stage; R: hydraulic radius; tau: bed shear stress; tau*: Shields number; u*: friction velocity; Re: Reynolds number; u: flow velocity from Manning's equation; Q: water discharge; q: water discharge per unit width.

Effects in no control works configuration

After the simulations and the calibration of the hydraulic parameters in clear water, we proceeded to set up a sandy bed to carry out the tests about the formation of the surface armoring and the overall sediment behavior upstream of the GCS after the flow. To start, a set of tests was carried out without inserting any transversal object, to use it as a reference / comparison situation with the scenario in which the GCSs are present.

The channel bed is made with desalinated marine sand, oxidized in order to eliminate all traces of organic matter. The material used was then sieved using the USDA ranges for sand with a metal sieve (mesh opening of 2 mm), in order to select the sandy fraction of the sediment, resulting in a 'mixture' of particles with a range of diameters between 0.2 and 2 mm. From the weighing tests the bulk density of the material used was 1320 kg m^{-3}. The sandy bottom was set up for a height equal to the threshold height of the weir placed at the canal closing section. Below are reported, at different longitudinal slope, the grain distribution curves for each run of the first set of experiments.

Slope = 0.31%

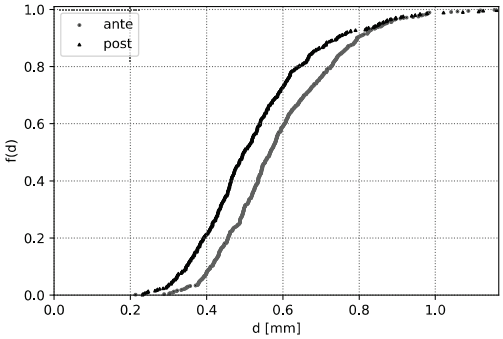

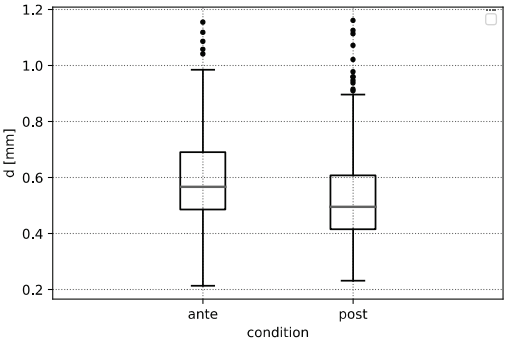

With a slope of 0.31% a general shift towards smaller grain diameters is observed. The d50 moves from 0.57 mm to 0.50 mm, while the d90 goes from 0.79 mm to 0.73 mm.

Slope = 0.62%

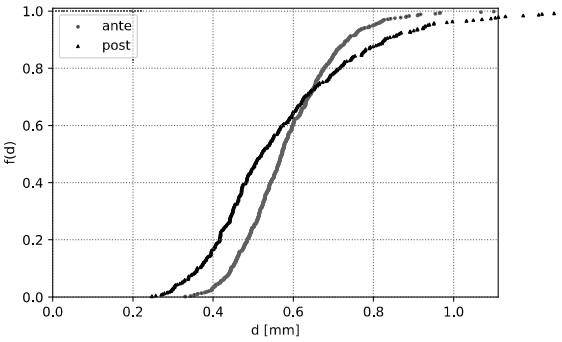

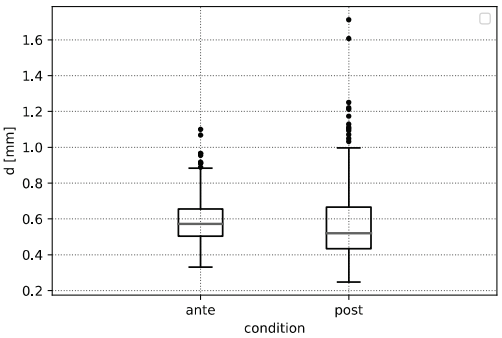

With a slope of 0.62% a general shift towards smaller grain diameters is observed. The d50 moves from 0.57 mm to 0.54 mm, while the d90 goes from 0.74 mm to 0.82 mm.

Slope = 0.94%

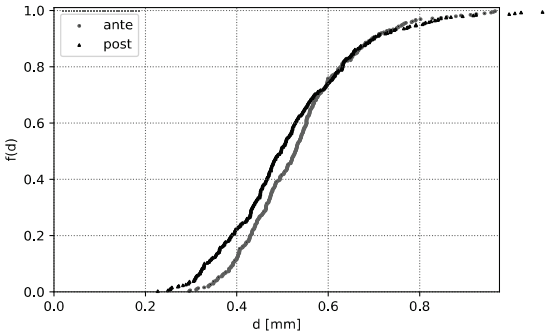

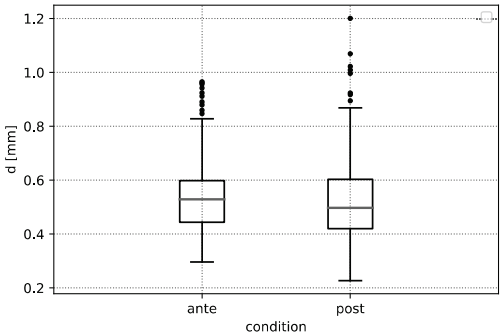

With a slope of 0.94% a general shift towards smaller grain diameters is observed. The d50 moves from 0.52 mm to 0.49 mm, while the d90 goes from 0.70 mm to 0.71 mm

Slope = 1.25%

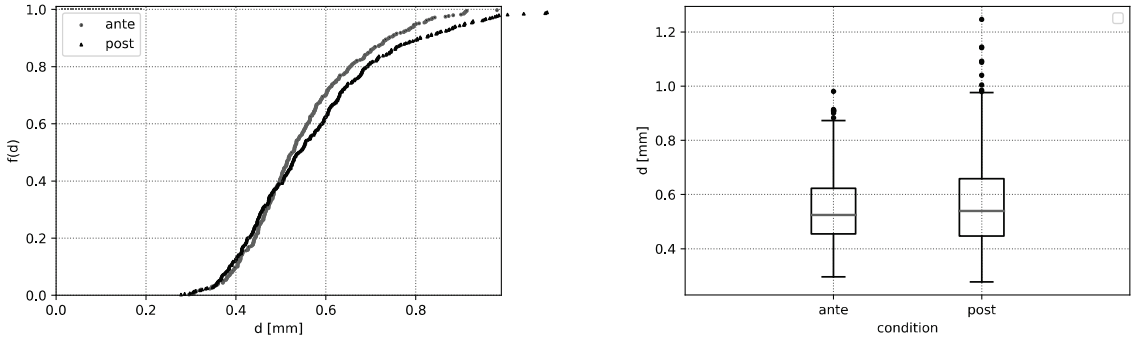

With a slope of 1.25% a first shift towards bigger grain diameters is observed. The d50 moves from 0.53 mm to 0.55 mm, while the d90 goes from 0.72 mm to 0.79 mm

Slope = 1.56%

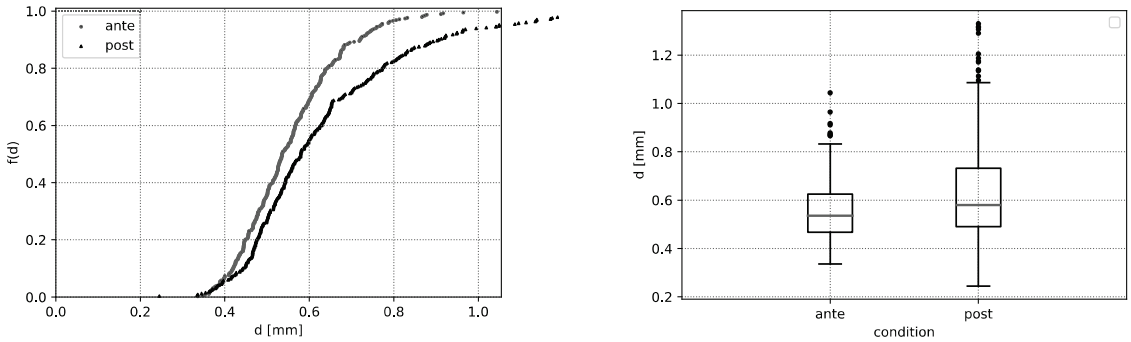

With a slope of 1.56% a general shift towards greater grain diameters is observed. The d50 moves from 0.54 mm to 0.60 mm, while the d90 goes from 0.71 mm to 0.87 mm

Slope = 1.88%

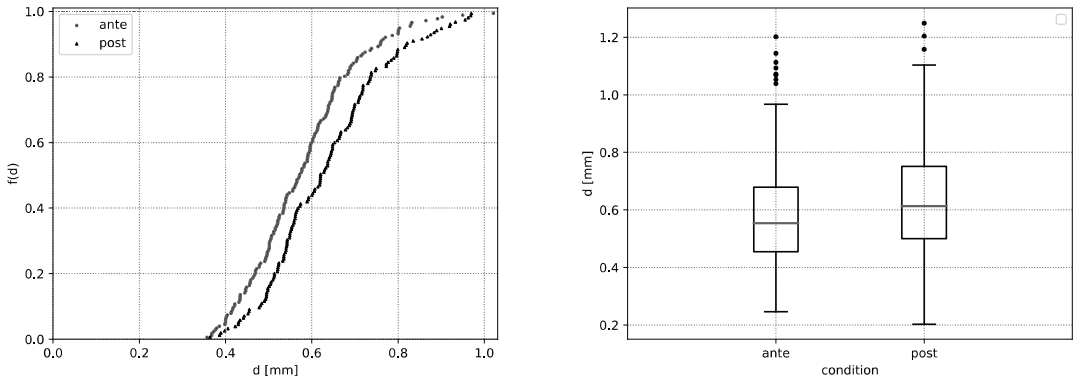

With a slope of 1.88% a general shift towards greater grain diameters is observed. The d50 moves from 0.53 mm to 0.55 mm, while the d90 remain equal to 0.72 mm

Image 11: Variation of the bed grain distribution, at different longitudinal slope, without GCS.

As can be seen from the data reported in Tables 3 and 4 and from the plot in Image 11, as the slope increases there is a progressive coarsening of the sand grains of the riverbed. Quantitatively, this process is paired to a progressive loss of the material (Table 3) forming the movable bed, which reaches 100% around the slope of 2% (the loss is 6.4% on average in all cases using GCSs).

Table 3: Bed material removed in the control area at different bed slopes

Total volume (cm^3)	Slope (%)	Removed volume (cm^3)	Removed percentage	Removed mass (g)
864	**0.31**	88	10.2%	116.2
	0.62	165	19.1%	217.8
	0.94	286	33.1%	377.5
	1.25	242	28.0%	319.4
	1.56	286	33.1%	377.5
	1.88	319	36.9%	421.1

Table 4: Percentile ratios after/before experiment: values smaller than one means diameter reduction, values greater than one means diameters coarsening

percentile/ condition	0.31_P	0.62_P	0.94_P	1.25_P	1.56_P	1.88_P
d5	0.84	0.76	0.86	0.97	0.97	1.01
d10	0.85	0.80	0.87	0.95	1.00	0.98
d15	0.84	0.81	0.90	0.98	1.02	0.99
d20	0.85	0.84	0.91	0.98	1.02	0.99
d25	0.85	0.86	0.91	0.98	1.06	1.04
d50	0.88	0.95	0.94	1.04	1.11	1.04
d55	0.88	0.95	0.94	1.04	1.13	1.03
d60	0.89	0.98	0.96	1.04	1.14	1.05
d65	0.89	0.98	0.96	1.05	1.14	1.04
d70	0.91	1.00	0.97	1.07	1.17	1.04
d75	0.90	1.02	0.98	1.05	1.18	1.04
d80	0.92	1.04	1.00	1.06	1.20	1.01
d85	0.91	1.09	1.00	1.07	1.21	0.99
d90	0.92	1.11	1.01	1.10	1.23	0.99
d95	0.94	1.16	1.04	1.12	1.28	0.97
d100	1.01	1.55	1.25	1.28	1.28	1.05

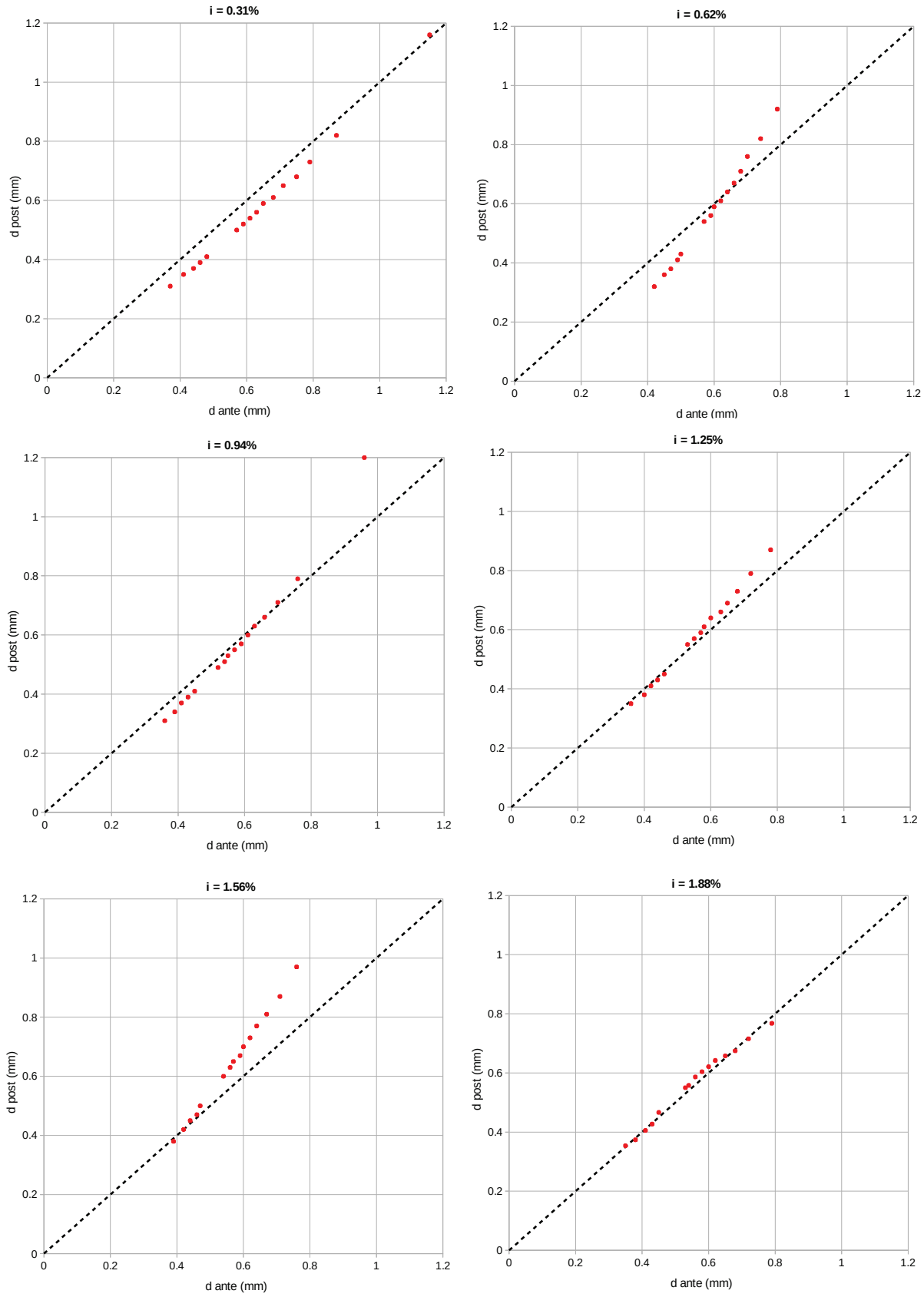

Image 12: Percentiles comparison of the sand bed, before and after the experiments without using any GCS

Effects in single grade control structure configuration

The GCS used has dimensions equal to (4 x 1.5 x 8) cm, with height equal to the initial one of the sandy bottom. It is placed at half length of the experimental channel, so as not to be affected by the turbulence created from the upstream tank and, at the same time, not to suffer the effects of the weir placed at the end of the flume.

The overall results of the first experiments indicate the formation of a dynamic armor coat (Little & Mayer, 1976), that depends on the bed slope and, unlike in the case of the formation of a static armor coat (in which finer elements are eroded) caused an increase in finer sediments percentage and a reduction of the larger ones.

Below are reported the plot related to the set of experiments:

Slope = 0.31%

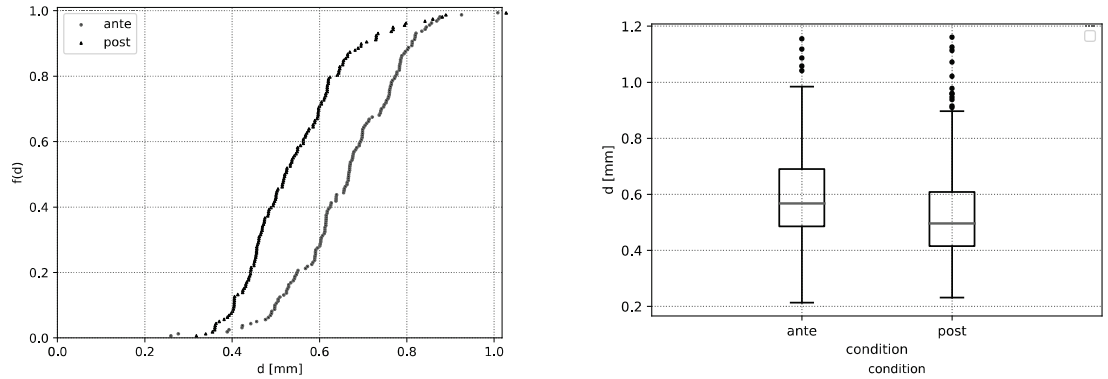

With a slope of 0.31% a general shift towards smaller grain diameters is observed. The d50 moves from 0.62 mm to 0.50 mm, while the d90 goes from 0.82 mm to 0.63 mm.

Slope = 0.62%

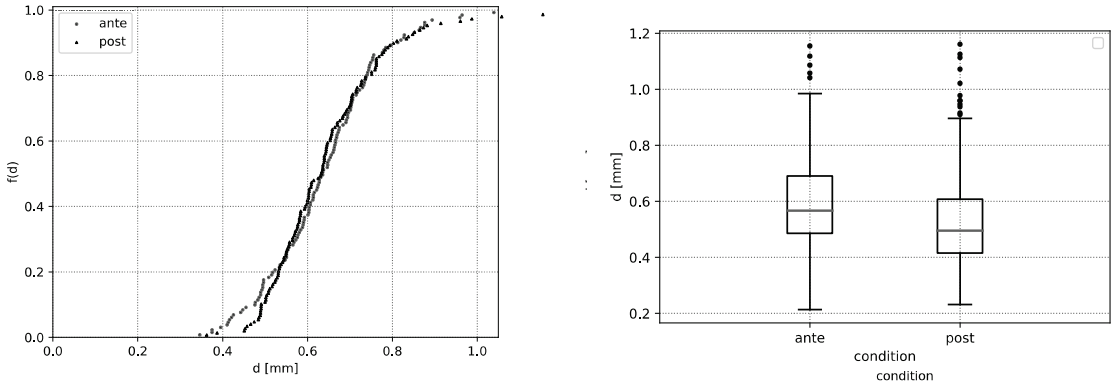

With a slope of 0.62% a there is no general change in the grain diameters observed. The d50 is in both cases equal to 0.63 mm, while the d90 is 0.81 mm.

Slope = 0.94%

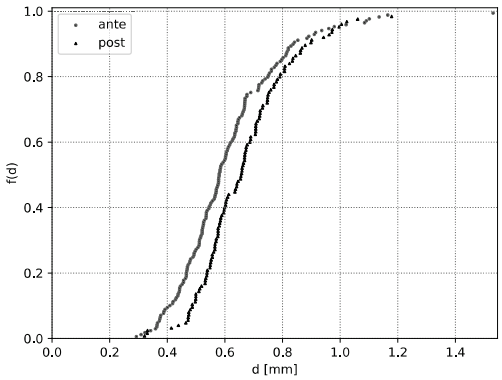

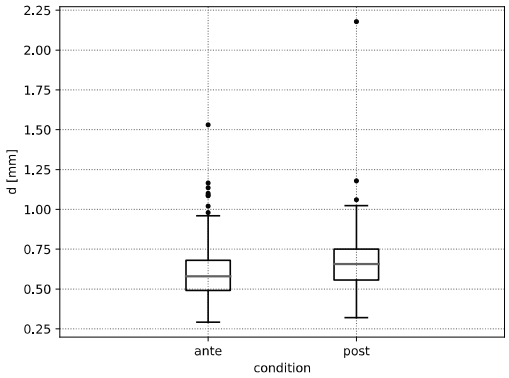

With a slope of 0.94% a general shift towards greater grain diameters is observed. The d50 moves from 0.58 mm to 0.66 mm, while the d90 goes from 0.83 mm to 0.88 mm.

Slope = 1.25%

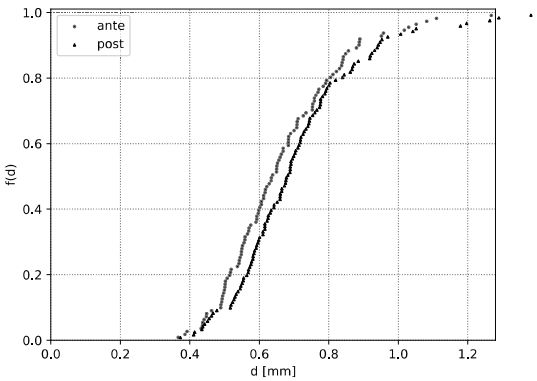

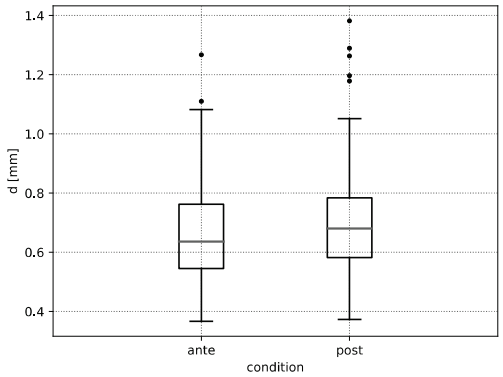

With a slope of 1.25% a general coarsening is observed. The d50 moves from 0.64 mm to 0.68 mm, while the d90 goes from 0.83 mm to 0.88 mm.

Slope = 1.56%

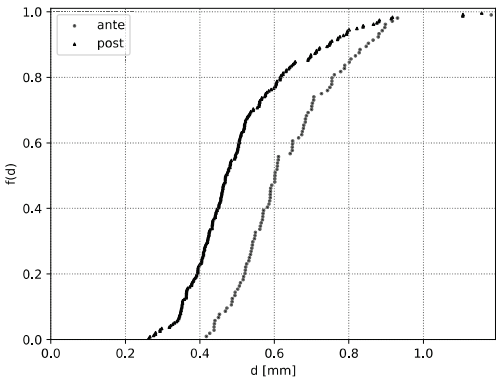

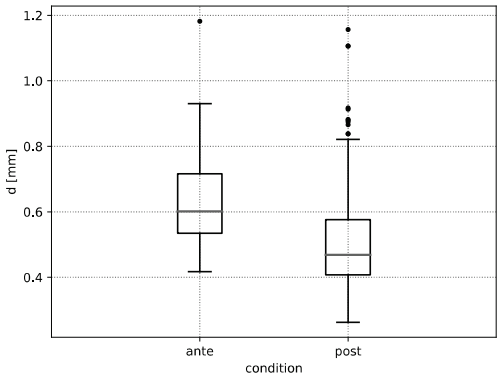

With a slope of 1.56% a general shift towards smaller diameters is observed. The d50 moves from 0.60 mm to 0.47 mm, while the d90 goes from 0.84 mm to 0.74 mm.

Slope = 1.88%

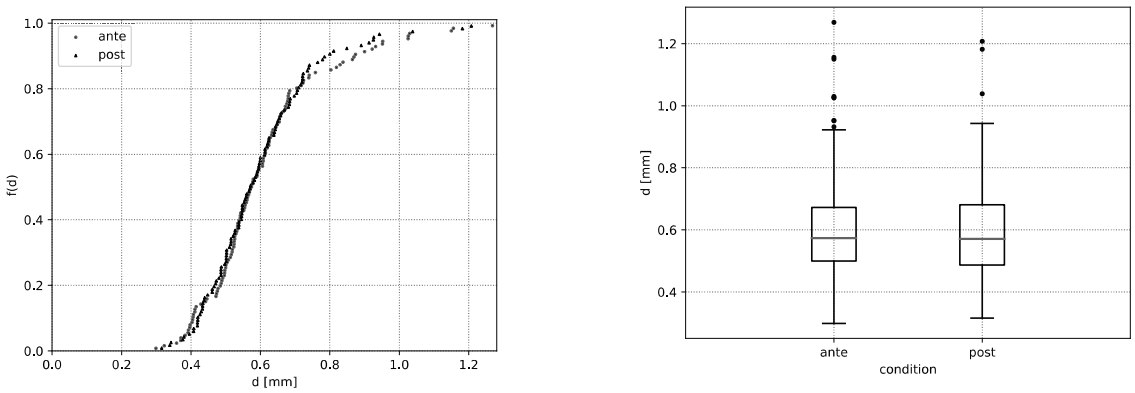

Image 13: Variation of the bed grain distribution, at different longitudinal slope, 1-GCS configuration

With a slope of 1.88% a there is no general change in the grain diameters observed. The d50 is in both cases equal to 0.57 mm, while the d90 goes from 0.87 to 0.78 mm.

Percentile relations and comparison with the no-GCS configuration…

The overall comparison of the sand grain distributions percentiles between the no-GCS and 1-GCS configuration (Image 14) highlights a bed grain coarsening for every slope, except for the slope of 1.56%, where finer grain are found. The average grain diameter increase is 25% (ranging from 7 to 35%) while the decrease, at the slope of 1.56%, is 20%. As shown in Image 15, higher increment happens in the first half of the distribution, whilst the increment in the second half is stable in each experiment.

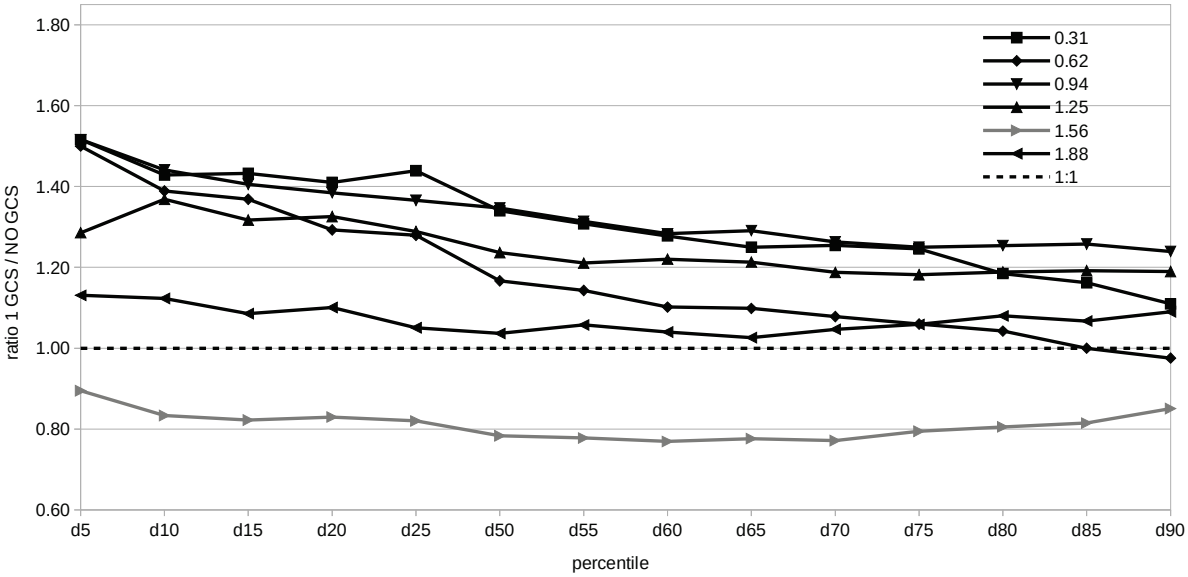

Image 14: General trend of the percentiles variation after the experiments between no-GCS and 1-GCS configuration

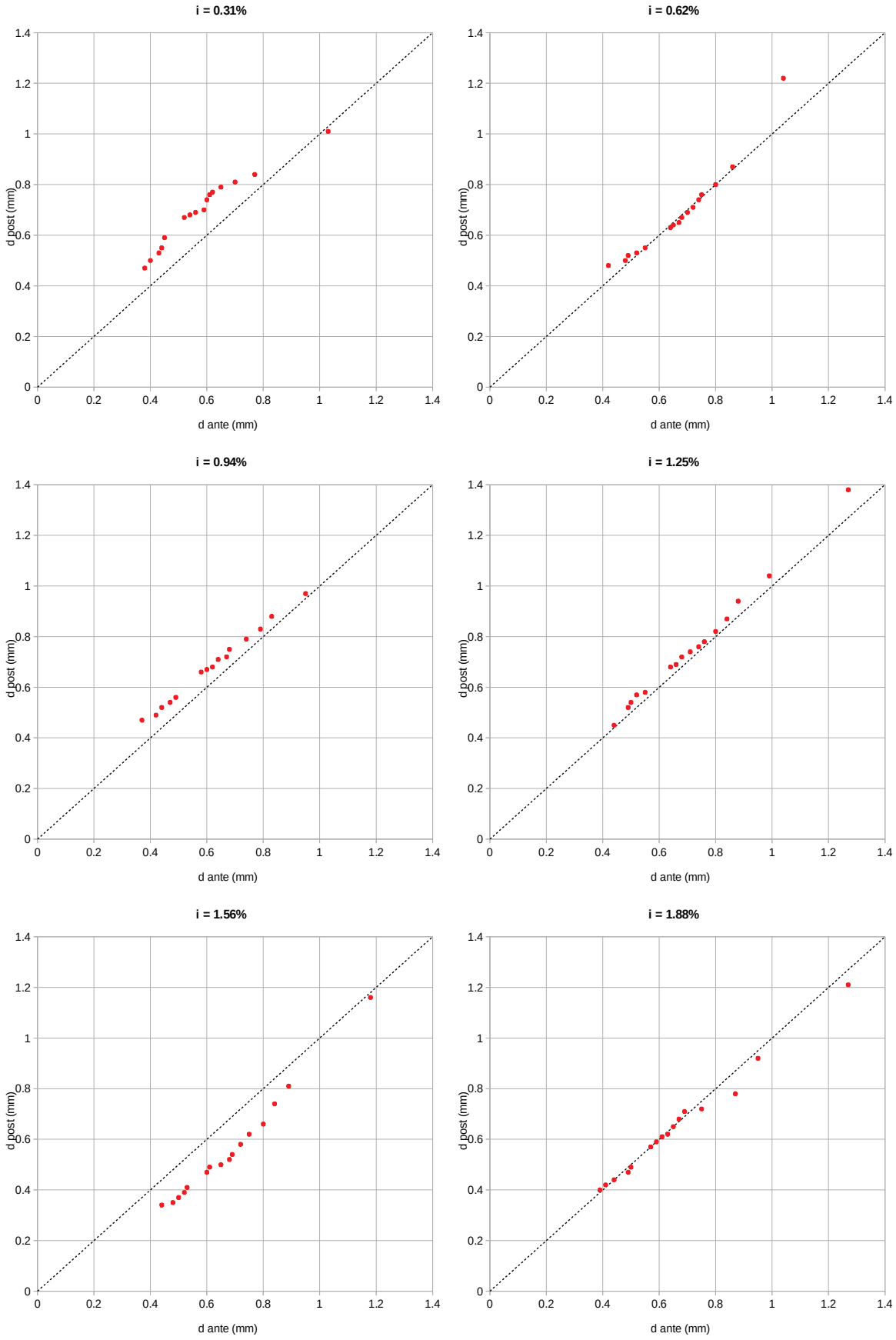

Image 15: Percentiles comparison of the sand grain diameters in no-GCS and 1-GCS configurations

Effects in three grade control structures configuration

The set of experiments was expanded by analyzing the granulometric curves of the sediment retained upstream of a three-GCS configuration, in steady flow condition and changing the bed slope value. In order to assess the effects on the riverbed of these structures, two interdistance values commonly used in the first approximation design were used, equal to $D = 1.5 \cdot H$ (6 cm, identified as configuration D6) and $D = 3 \cdot H$ (12 cm, identified as configuration D12), with H height of the GCSs (4 cm). Image 16 shows the general configuration.

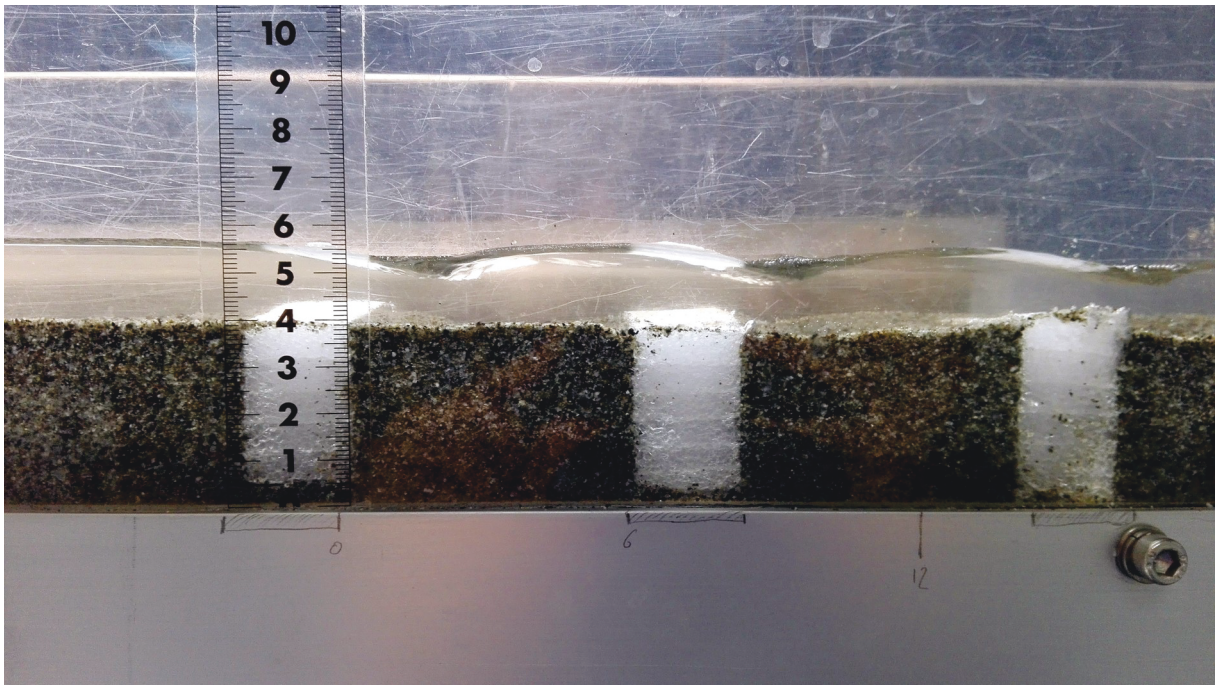

Image 16: Overwiev of the 3-GCS configuration

Below are reported the plot related to the set of experiments:

Each of the following tables contains, measured in millimiters, the grains diameter measurements taken before the experiment (A), after the experiment (P) and the non-dimensional ratio of the remaining sediment compared with the initial one. This ratio quickly allow to understand if the diameters of sand grains at the end of the experiment are finer (ratio < 1) or coarser (ratio > 1) compared to the initial conditions. The numbering of the control areas goes from the upstream stilling reservoir towards the flume outlet.

Table 5: Three-GCS, distance 1 runs. Characteristic diameters distribution (mm) (follow on next page)

percentile/ condition	0.31_6 1A	0.31_6 2A	0.31_6 3A	0.31_6 1P	0.31_6 2P	0.31_6 3P	0.31_6 1 ratio	0.31_6 2 ratio	0.31_6 3 ratio
d5	0.59	0.57	0.52	0.69	0.58	0.52	1.17	1.02	1.00
d10	0.64	0.62	0.56	0.74	0.64	0.57	1.16	1.03	1.02
d15	0.68	0.65	0.59	0.77	0.68	0.61	1.13	1.05	1.03
d20	0.71	0.68	0.61	0.80	0.71	0.64	1.13	1.04	1.05
d25	0.73	0.70	0.63	0.83	0.74	0.67	1.14	1.06	1.06
d50	0.85	0.81	0.72	0.95	0.88	0.80	1.12	1.09	1.11
d55	0.87	0.83	0.74	0.97	0.91	0.83	1.11	1.10	1.12
d60	0.90	0.86	0.76	1.00	0.94	0.86	1.11	1.09	1.13
d65	0.92	0.88	0.78	1.02	0.98	0.89	1.11	1.11	1.14
d70	0.95	0.91	0.80	1.05	1.01	0.92	1.11	1.11	1.15
d75	0.98	0.94	0.82	1.08	1.05	0.96	1.10	1.12	1.17
d80	1.02	0.97	0.85	1.12	1.10	1.01	1.10	1.13	1.19
d85	1.07	1.01	0.88	1.16	1.15	1.06	1.08	1.14	1.20
d90	1.12	1.06	0.93	1.22	1.23	1.13	1.09	1.16	1.22
d95	1.22	1.15	0.99	1.31	1.35	1.25	1.07	1.17	1.26
d100	1.39	1.37	1.20	1.70	2.00	1.94	1.22	1.46	1.62

percentile/ condition	0.62_6 1A	0.62_6 2A	0.62_6 3A	0.62_6 1P	0.62_6 2P	0.62_6 3P	0.62_6 1 ratio	0.62_6 2 ratio	0.62_6 3 ratio
d5	0.38	0.37	0.31	0.49	0.35	0.28	1.29	0.95	0.90
d10	0.41	0.40	0.34	0.52	0.38	0.32	1.27	0.95	0.94
d15	0.43	0.42	0.36	0.54	0.41	0.35	1.26	0.98	0.97
d20	0.45	0.44	0.37	0.56	0.43	0.37	1.24	0.98	1.00
d25	0.46	0.45	0.39	0.57	0.45	0.39	1.24	1.00	1.00
d50	0.52	0.52	0.45	0.64	0.54	0.49	1.23	1.04	1.09
d55	0.54	0.53	0.46	0.65	0.56	0.52	1.20	1.06	1.13
d60	0.55	0.55	0.47	0.67	0.58	0.54	1.22	1.05	1.15
d65	0.56	0.56	0.49	0.68	0.60	0.56	1.21	1.07	1.14
d70	0.58	0.58	0.50	0.70	0.63	0.59	1.21	1.09	1.18
d75	0.60	0.59	0.52	0.72	0.65	0.62	1.20	1.10	1.19
d80	0.62	0.62	0.54	0.74	0.68	0.66	1.19	1.10	1.22
d85	0.64	0.64	0.56	0.76	0.72	0.71	1.19	1.13	1.27
d90	0.67	0.67	0.60	0.79	0.77	0.77	1.18	1.15	1.28
d95	0.72	0.72	0.65	0.84	0.85	0.87	1.17	1.18	1.34
d100	1.05	0.94	0.81	1.04	1.10	1.36	0.99	1.17	1.68

percentile/ condition	0.94_6 1A	0.94_6 2A	0.94_6 3A	0.94_6 1P	0.94_6 2P	0.94_6 3P	0.94_6 1 ratio	0.94_6 2 ratio	0.94_6 3 ratio
d5	0.27	0.30	0.30	0.18	0.22	0.27	0.67	0.73	0.90
d10	0.30	0.33	0.33	0.20	0.26	0.31	0.67	0.79	0.94
d15	0.32	0.35	0.35	0.21	0.28	0.33	0.66	0.80	0.94
d20	0.33	0.37	0.36	0.23	0.31	0.35	0.70	0.84	0.97
d25	0.34	0.38	0.38	0.24	0.33	0.37	0.71	0.87	0.97
d50	0.40	0.45	0.45	0.30	0.43	0.46	0.75	0.96	1.02
d55	0.42	0.47	0.46	0.31	0.45	0.48	0.74	0.96	1.04
d60	0.43	0.48	0.48	0.32	0.47	0.50	0.74	0.98	1.04
d65	0.44	0.50	0.49	0.34	0.49	0.52	0.77	0.98	1.06
d70	0.46	0.52	0.51	0.35	0.52	0.55	0.76	1.00	1.08
d75	0.48	0.54	0.53	0.37	0.55	0.57	0.77	1.02	1.08
d80	0.50	0.56	0.55	0.39	0.59	0.60	0.78	1.05	1.09
d85	0.52	0.59	0.58	0.41	0.63	0.64	0.79	1.07	1.10
d90	0.55	0.62	0.61	0.44	0.70	0.70	0.80	1.13	1.15
d95	0.60	0.68	0.67	0.50	0.80	0.78	0.83	1.18	1.16
d100	0.95	0.85	0.99	0.87	1.41	1.49	0.92	1.66	1.51

percentile/ condition	1.56_6 1A	1.56_6 2A	1.56_6 3A	1.56_6 1P	1.56_6 2P	1.56_6 3P	1.56_6 1 ratio	1.56_6 2 ratio	1.56_6 3 ratio
d5	0.31	0.31	0.31	0.29	0.27	0.30	0.94	0.87	0.97
d10	0.34	0.34	0.34	0.32	0.31	0.35	0.94	0.91	1.03
d15	0.36	0.36	0.36	0.34	0.34	0.37	0.94	0.94	1.02
d20	0.38	0.38	0.38	0.36	0.37	0.39	0.95	0.97	1.02
d25	0.39	0.40	0.39	0.38	0.39	0.41	0.97	0.98	1.05
d50	0.47	0.47	0.47	0.45	0.50	0.51	0.96	1.06	1.09
d55	0.48	0.48	0.48	0.47	0.52	0.53	0.98	1.08	1.11
d60	0.50	0.50	0.50	0.49	0.54	0.56	0.98	1.08	1.11
d65	0.51	0.52	0.51	0.50	0.57	0.58	0.98	1.10	1.13
d70	0.53	0.53	0.53	0.52	0.60	0.61	0.98	1.13	1.15
d75	0.55	0.55	0.55	0.55	0.63	0.63	1.00	1.15	1.15
d80	0.57	0.58	0.58	0.57	0.67	0.67	1.00	1.16	1.15
d85	0.60	0.61	0.60	0.61	0.72	0.71	1.02	1.18	1.18
d90	0.64	0.64	0.64	0.65	0.79	0.78	1.02	1.23	1.21
d95	0.70	0.71	0.71	0.72	0.90	0.87	1.03	1.27	1.22
d100	1.03	1.07	0.98	1.19	1.55	1.65	1.16	1.45	1.69

percentile/ condition	1.87_6 1A	1.87_6 2A	1.87_6 3A	1.87_6 1P	1.87_6 2P	1.87_6 3P	1.87_6 1 ratio	1.87_6 2 ratio	1.87_6 3 ratio
d5	0.29	0.32	0.33	0.35	0.29	0.28	1.21	0.91	0.85
d10	0.33	0.35	0.37	0.39	0.34	0.31	1.18	0.97	0.84
d15	0.35	0.37	0.39	0.41	0.37	0.34	1.17	1.00	0.87
d20	0.37	0.39	0.41	0.44	0.40	0.37	1.19	1.03	0.90
d25	0.39	0.41	0.43	0.46	0.42	0.39	1.18	1.02	0.91
d50	0.48	0.49	0.52	0.56	0.55	0.50	1.17	1.12	0.96
d55	0.49	0.50	0.54	0.58	0.57	0.53	1.18	1.14	0.98
d60	0.51	0.52	0.56	0.60	0.60	0.55	1.18	1.15	0.98
d65	0.53	0.54	0.58	0.63	0.63	0.58	1.19	1.17	1.00
d70	0.56	0.56	0.60	0.65	0.66	0.61	1.16	1.18	1.02
d75	0.58	0.58	0.62	0.68	0.70	0.64	1.17	1.21	1.03
d80	0.61	0.61	0.65	0.72	0.75	0.68	1.18	1.23	1.05
d85	0.65	0.64	0.69	0.76	0.80	0.73	1.17	1.25	1.06
d90	0.70	0.68	0.74	0.82	0.88	0.80	1.17	1.29	1.08
d95	0.78	0.75	0.81	0.91	1.01	0.92	1.17	1.35	1.14
d100	1.17	1.04	1.00	1.51	1.64	1.56	1.29	1.58	1.56

percentile/ condition	2.19_6 1A	2.19_6 2A	2.19_6 3A	2.19_12 1P	2.19_12 2P	2.19_12 3P	2.19_12 1 ratio	2.19_12 2 ratio	2.19_12 3 ratio
d5	0.30	0.33	0.32	0.22	0.26	0.28	0.73	0.78	0.87
d10	0.33	0.36	0.35	0.25	0.29	0.32	0.76	0.81	0.91
d15	0.35	0.38	0.37	0.28	0.32	0.34	0.79	0.83	0.93
d20	0.37	0.40	0.39	0.29	0.33	0.37	0.79	0.83	0.94
d25	0.39	0.42	0.40	0.31	0.35	0.38	0.79	0.83	0.96
d50	0.46	0.50	0.47	0.39	0.43	0.48	0.85	0.86	1.03
d55	0.48	0.51	0.49	0.41	0.44	0.51	0.85	0.87	1.03
d60	0.50	0.53	0.51	0.43	0.46	0.53	0.86	0.87	1.04
d65	0.52	0.55	0.52	0.45	0.49	0.56	0.86	0.88	1.07
d70	0.53	0.57	0.54	0.47	0.50	0.58	0.89	0.88	1.07
d75	0.56	0.59	0.56	0.50	0.53	0.61	0.89	0.89	1.09
d80	0.58	0.62	0.58	0.53	0.56	0.65	0.91	0.90	1.11
d85	0.61	0.65	0.61	0.56	0.59	0.69	0.92	0.91	1.12
d90	0.66	0.69	0.65	0.61	0.64	0.75	0.93	0.93	1.16
d95	0.72	0.76	0.71	0.69	0.71	0.85	0.96	0.94	1.20
d100	1.01	0.98	0.83	1.04	1.21	1.34	1.03	1.24	1.61

Table 6: Three-GCS, distance 2 runs. Characteristic diameters distribution (mm) (follow on next page)

percentile/ condition	0.31_12 1A	0.31_12 2A	0.31_12 3A	0.31_12 1P	0.31_12 2P	0.31_12 3P	0.31_12 1 ratio	0.31_12 2 ratio	0.31_12 3 ratio
d5	0.42	0.45	0.43	0.43	0.29	0.35	1.03	0.64	0.81
d10	0.45	0.48	0.47	0.47	0.32	0.38	1.05	0.67	0.81
d15	0.47	0.50	0.49	0.50	0.34	0.40	1.07	0.68	0.82
d20	0.49	0.52	0.51	0.52	0.36	0.42	1.06	0.69	0.82
d25	0.51	0.54	0.53	0.54	0.37	0.44	1.06	0.69	0.83
d50	0.57	0.62	0.60	0.61	0.44	0.51	1.07	0.71	0.85
d55	0.59	0.63	0.62	0.62	0.46	0.53	1.05	0.73	0.85
d60	0.60	0.65	0.63	0.64	0.47	0.54	1.06	0.72	0.86
d65	0.62	0.67	0.65	0.65	0.49	0.56	1.05	0.73	0.86
d70	0.63	0.68	0.67	0.67	0.51	0.58	1.06	0.75	0.87
d75	0.65	0.70	0.69	0.68	0.53	0.60	1.05	0.76	0.87
d80	0.67	0.73	0.71	0.70	0.55	0.62	1.05	0.75	0.87
d85	0.69	0.76	0.74	0.73	0.58	0.65	1.05	0.76	0.88
d90	0.73	0.79	0.77	0.76	0.62	0.69	1.04	0.78	0.90
d95	0.78	0.85	0.83	0.80	0.68	0.75	1.03	0.80	0.90
d100	1.01	1.16	0.97	1.09	1.15	1.20	1.08	0.99	1.24

percentile/ condition	0.62_12 1A	0.62_12 2A	0.62_12 3A	0.62_12 1P	0.62_12 2P	0.62_12 3P	0.62_12 1 ratio	0.62_12 2 ratio	0.62_12 3 ratio
d5	0.37	0.41	0.38	0.32	0.35	0.29	0.86	0.85	0.76
d10	0.40	0.44	0.41	0.36	0.39	0.33	0.90	0.89	0.80
d15	0.42	0.46	0.44	0.38	0.42	0.35	0.90	0.91	0.80
d20	0.44	0.48	0.46	0.40	0.44	0.38	0.91	0.92	0.83
d25	0.46	0.50	0.47	0.42	0.46	0.40	0.91	0.92	0.85
d50	0.53	0.56	0.55	0.51	0.56	0.50	0.96	1.00	0.91
d55	0.55	0.58	0.57	0.53	0.58	0.52	0.96	1.00	0.91
d60	0.56	0.59	0.58	0.55	0.60	0.54	0.98	1.02	0.93
d65	0.58	0.61	0.60	0.57	0.62	0.57	0.98	1.02	0.95
d70	0.60	0.62	0.62	0.59	0.64	0.60	0.98	1.03	0.97
d75	0.62	0.64	0.64	0.62	0.67	0.63	1.00	1.05	0.98
d80	0.64	0.66	0.67	0.65	0.70	0.66	1.02	1.06	0.99
d85	0.67	0.69	0.70	0.68	0.74	0.71	1.01	1.07	1.01
d90	0.71	0.72	0.73	0.73	0.80	0.77	1.03	1.11	1.05
d95	0.77	0.77	0.80	0.81	0.88	0.86	1.05	1.14	1.08
d100	0.94	0.91	1.20	1.14	1.39	1.38	1.21	1.53	1.15

percentile/ condition	0.94_12 1A	0.94_12 2A	0.94_12 3A	0.94_12 1P	0.94_12 2P	0.94_12 3P	0.94_12 1 ratio	0.94_12 2 ratio	0.94_12 3 ratio
d5	0.30	0.33	0.30	0.25	0.25	0.27	0.83	0.76	0.90
d10	0.33	0.36	0.33	0.28	0.30	0.32	0.85	0.83	0.97
d15	0.35	0.38	0.35	0.30	0.33	0.35	0.86	0.87	1.00
d20	0.36	0.40	0.36	0.32	0.36	0.38	0.89	0.90	1.06
d25	0.38	0.42	0.38	0.33	0.39	0.41	0.87	0.93	1.08
d50	0.45	0.49	0.44	0.41	0.52	0.54	0.91	1.06	1.23
d55	0.47	0.51	0.45	0.42	0.55	0.57	0.89	1.08	1.27
d60	0.48	0.52	0.47	0.44	0.58	0.60	0.92	1.12	1.28
d65	0.50	0.54	0.48	0.46	0.61	0.63	0.92	1.13	1.31
d70	0.51	0.56	0.50	0.48	0.65	0.67	0.94	1.16	1.34
d75	0.53	0.58	0.51	0.50	0.70	0.71	0.94	1.21	1.39
d80	0.56	0.60	0.53	0.53	0.75	0.77	0.95	1.25	1.45
d85	0.59	0.63	0.56	0.56	0.81	0.83	0.95	1.29	1.48
d90	0.62	0.67	0.59	0.60	0.91	0.92	0.97	1.36	1.56
d95	0.68	0.73	0.64	0.67	1.06	1.07	0.99	1.45	1.67
d100	0.98	1.23	0.76	0.96	1.49	1.40	0.98	1.21	1.84

percentile/ condition	1.56_12 1A	1.56_12 2A	1.56_12 3A	1.56_12 1P	1.56_12 2P	1.56_12 3P	1.56_12 1 ratio	1.56_12 2 ratio	1.56_12 3 ratio
d5	0.29	0.33	0.34	0.29	0.29	0.21	1.00	0.88	0.62
d10	0.33	0.37	0.38	0.32	0.33	0.25	0.97	0.89	0.66
d15	0.35	0.39	0.40	0.35	0.36	0.27	1.00	0.92	0.68
d20	0.37	0.41	0.42	0.37	0.39	0.32	1.00	0.95	0.75
d25	0.39	0.43	0.45	0.40	0.42	0.35	1.03	0.98	0.77
d50	0.47	0.51	0.54	0.50	0.54	0.43	1.06	1.06	0.79
d55	0.49	0.52	0.56	0.52	0.56	0.45	1.06	1.08	0.80
d60	0.51	0.54	0.58	0.54	0.59	0.45	1.06	1.09	0.78
d65	0.53	0.56	0.60	0.57	0.62	0.45	1.08	1.11	0.76
d70	0.55	0.58	0.63	0.59	0.65	0.51	1.07	1.12	0.81
d75	0.57	0.60	0.65	0.62	0.69	0.53	1.09	1.15	0.82
d80	0.60	0.63	0.68	0.66	0.73	0.55	1.10	1.16	0.81
d85	0.64	0.66	0.72	0.70	0.79	0.63	1.09	1.20	0.87
d90	0.68	0.70	0.78	0.77	0.87	0.68	1.13	1.24	0.87
d95	0.76	0.77	0.86	0.87	0.99	0.80	1.14	1.29	0.93
d100	1.24	0.98	1.15	1.35	1.59	1.02	1.09	1.62	0.89

percentile/ condition	1.87_12 1A	1.87_12 2A	1.87_12 3A	1.87_12 1P	1.87_12 2P	1.87_12 3P	1.87_12 1 ratio	1.87_12 2 ratio	1.87_12 3 ratio
d5	0.33	0.38	0.41	0.30	0.31	0.30	0.91	0.82	0.73
d10	0.36	0.41	0.44	0.34	0.36	0.33	0.94	0.88	0.75
d15	0.39	0.43	0.46	0.38	0.39	0.35	0.97	0.91	0.76
d20	0.41	0.45	0.48	0.41	0.42	0.37	1.00	0.93	0.77
d25	0.43	0.47	0.50	0.43	0.44	0.39	1.00	0.94	0.78
d50	0.51	0.54	0.57	0.56	0.56	0.47	1.10	1.04	0.82
d55	0.53	0.56	0.58	0.58	0.59	0.49	1.09	1.05	0.84
d60	0.54	0.57	0.60	0.61	0.61	0.51	1.13	1.07	0.85
d65	0.56	0.59	0.62	0.64	0.64	0.52	1.14	1.08	0.84
d70	0.58	0.61	0.63	0.68	0.67	0.55	1.17	1.10	0.87
d75	0.61	0.63	0.65	0.72	0.71	0.57	1.18	1.13	0.88
d80	0.64	0.65	0.67	0.76	0.75	0.60	1.19	1.15	0.90
d85	0.67	0.68	0.70	0.82	0.81	0.63	1.22	1.19	0.90
d90	0.71	0.72	0.74	0.90	0.88	0.67	1.27	1.22	0.91
d95	0.79	0.78	0.79	1.03	1.00	0.75	1.30	1.28	0.95
d100	1.20	1.01	1.05	1.82	1.72	0.98	1.52	1.70	0.93

percentile/ condition	2.19_6 1P	2.19_6 2P	2.19_6 3P	2.19_12 1P	2.19_12 2P	2.19_12 3P	2.19_12 1 ratio	2.19_12 2 ratio	2.19_12 3 ratio
d5	0.29	0.34	0.36	0.27	0.32	0.34	0.93	0.94	0.94
d10	0.33	0.39	0.40	0.31	0.36	0.39	0.94	0.92	0.98
d15	0.36	0.42	0.44	0.34	0.39	0.42	0.94	0.93	0.95
d20	0.39	0.45	0.47	0.36	0.41	0.45	0.92	0.91	0.96
d25	0.41	0.47	0.50	0.38	0.43	0.47	0.93	0.91	0.94
d50	0.53	0.59	0.63	0.48	0.53	0.59	0.91	0.90	0.94
d55	0.55	0.62	0.65	0.50	0.55	0.62	0.91	0.89	0.95
d60	0.58	0.65	0.68	0.53	0.57	0.65	0.91	0.88	0.96
d65	0.61	0.68	0.72	0.55	0.60	0.68	0.90	0.88	0.94
d70	0.64	0.71	0.75	0.58	0.62	0.71	0.91	0.87	0.95
d75	0.68	0.75	0.79	0.61	0.65	0.75	0.90	0.87	0.95
d80	0.72	0.79	0.84	0.65	0.69	0.79	0.90	0.87	0.94
d85	0.77	0.84	0.90	0.69	0.73	0.84	0.90	0.87	0.93
d90	0.85	0.91	0.97	0.75	0.79	0.92	0.88	0.87	0.95
d95	0.97	1.03	1.11	0.85	0.88	1.04	0.88	0.85	0.94
d100	1.77	1.60	1.52	1.28	1.50	1.64	0.72	0.94	1.08

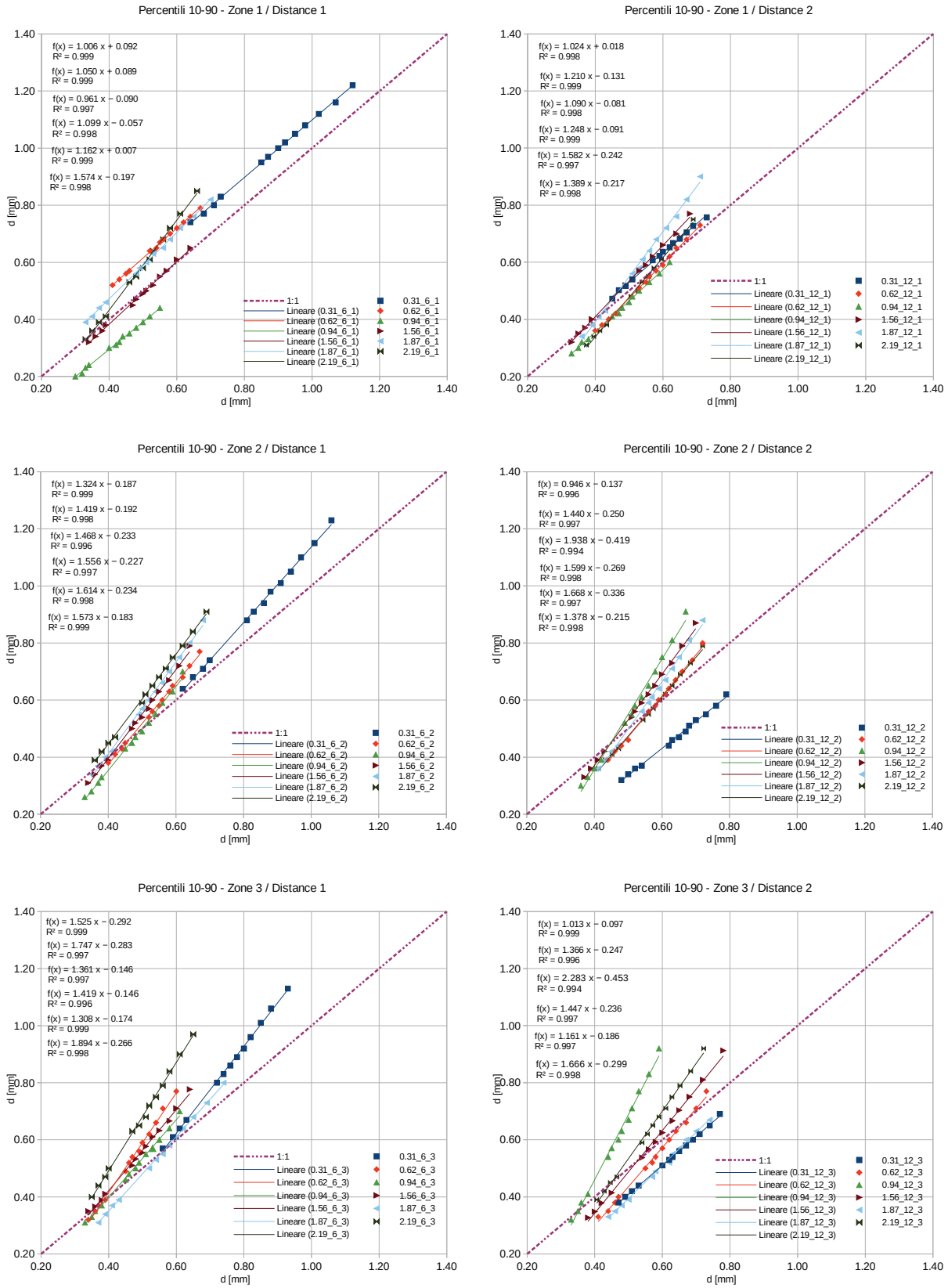

Image 17: Comparison between dx_{post} (Y axis) and dx_{ante} (X axis) for different bed slopes, 3-GCS configuration, distance 1 (left side) and distance 2 (right side)

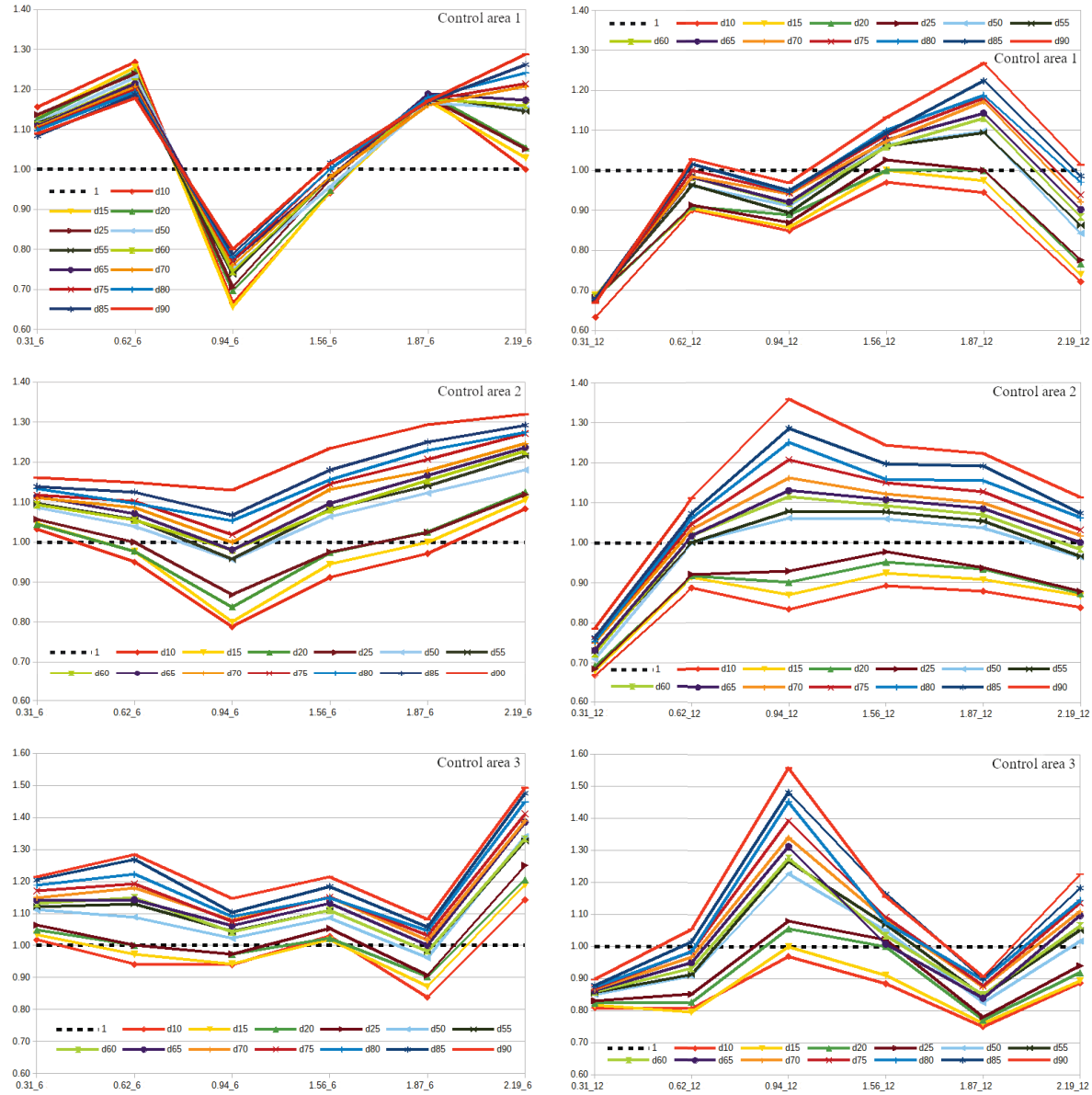

Image 18: Ratio dx_{post}/dx_{ante} at different bed slopes, 3-GCS configuration, distance 1 (left side) and distance 2 (right side)

The plots in Image 17 and 18 highlight different behaviours in each combination of distance and bed longitudinal slope, showing a clear shift towards larger grain diameters. In particular:

- the 0.94% slope is overall the most sensitive one in terms of grain size spread in almost all run except for the *Distance_1–GCS_3* where the general trend is regular, except for the slope of 2.2%, where a significant shift towards coarser diameters is detected;
- at the *Distance_1–GCS_1* combination the percentile spread at different bed slopes is the least of all simulation. This suggest a relative stability of this configuration at different slope values, while when GCS are further each other, upstream of them there is a tendency to select coarser grain, in particular at high bed slopes;
- both *Distance_1–GCS_2* and *Distance_2–GCS_2* combinations have the widest dx_{post}/dx_{ante} spread at different bed slopes (with a maximum at i = 0.94%), which represent a higher susceptibility to channel bed modification. In these two configuration, a general fining can be observed up to the 25^{th} percentile of the diameters distribution while grain diameters from 25^{th} to 95^{th} percentile tends to become coarser;
- at *Distance_1–GCS_3* configuration grains slowly tend to shrink (except for the highest slope were coarser sand is selected) while in *Distance_2–GCS_3* the 0.94% slope causes an anomalous wide spread).

To highlight the presence of statistically significant differences between the bed grain size distributions in 1-GCS and 3-GCS configurations, the two tails non-parametric Kolmogorov-Smirnov test was used. This is one of the most useful and non-parametric methods for comparing two samples, as it is sensitive to differences in both location and shape of the empirical cumulative distribution functions of the two samples. The KS statistic quantifies the distance between the two empirical distribution of the two samples compared. The null hypothesis H0 is that the samples are drawn from the same distribution.

As can be seen in Table 7, at different slope, the KS test confirm the presence of more statistically significant differences (identified with p-value < 0.05) between the 3-GCS (left side) and 1-GCS (right side) scenarios at the shortest distance (8 positive cases out of 15 at the shorter distance, against 3 positive cases out of 15 at greater distance). This suggest that greater relative inter-operam influence may be due to different pattern in energy dissipation in correspondence of the three critical status, and that this interaction lose magnitude at a greater distance.

Table 7: p-values related to the Kolmogorov-Smirnov tests carried out to test the presence of statistically significant differences between the granulometric curve (values lesser than 0.05 indicate to reject the null hypothesis of equal distributions)

Configuration	Slope	Distance	GCS	1 GCS				
	%	cm	n.	0.31	0.62	0.94	1.56	1.88
3GCS	0.31	6	1	**< 0.05**				
	0.62				> 0.05			
	0.94					**< 0.05**		
	1.56						> 0.05	
	1.88							> 0.05
	0.31		2	**< 0.05**				
	0.62				> 0.05			
	0.94					**< 0.05**		
	1.56						**< 0.05**	
	1.88							**< 0.05**
	0.31		3	**< 0.05**				
	0.62				> 0.05			
	0.94					**< 0.05**		
	1.56						> 0.05	
	1.88							> 0.05
	0.31	12	1	> 0.05				
	0.62				> 0.05			
	0.94					**< 0.05**		
	1.56						> 0.05	
	1.88							> 0.05
	0.31		2	**< 0.05**				
	0.62				> 0.05			
	0.94					> 0.05		
	1.56						> 0.05	
	1.88							> 0.05
	0.31		3	**< 0.05**				
	0.62				> 0.05			
	0.94					> 0.05		
	1.56						> 0.05	
	1.88							> 0.05

CONCLUSION AND FUTURE PERSPECTIVES

The knowledge of erosion and sediment transport mechanics is important to control the evolutionary processes of torrents, and hydraulic structures can modifies their natural evolution, and can propagate at distance. In order to propose a contribution to a better understanding of these phenomena, the aim of this study was to evaluate, on a physical model at a laboratory scale, the effects of grade control works in a river. Therefore, under steady-flow conditions, the behavior of a non-uniform sandy bed was analyzed at different longitudinal slopes in a laboratory channel.

In some sets of experiments and in particular in those with three GCS in series, already at a macroscopic level, the formation of an armoring layer was found. This layer "shields" the finest particles from the shear action of the water, giving stability to the riverbed. The particles that form this layer indeed require more energy to be removed, being larger in size and often arranged in "clusters" which add further consistency to the aggregates. In the same set of simulations, a much lower eroded volume than in the other simulations (on average 6.5% instead of 10-37%) is detected; this further confirms that the fine component of the sediment is not removed from the control area but, consistently with the theory of the armoring, it moves slowly under the surface remaining available on site.

Obtained results indicate that at higher gradients ($i > 1\%$) the close range three-GCSs configuration (which is similar to what in naturalistic engineering is known as step-pool configuration) is more suitable to facilitate the formation of the armoring. At slope of less than 1%, three close GCSs could cause a fining of the riverbed, with a consequent increase in the possibility of erosion at changes in flow conditions. On the other hand, at lower slope, the configuration with only one GCS helps the formation of a superficial armoring layer but, also after the statistical tests carried out, it is clear that the effect is equally obtainable by increasing the distance between the GCSs. With the same effects obtained, the adoption of a configuration with three GCSs is however preferable, compared to the single-control work configuration, as it offers numerous technical and non-technical advantages:

- each of the three GCS in sequence contributes for a fraction of the total correction required, having a reciprocal influence and receiving a portion of the structural stresses, resulting overall more solid than a single GCS;
- as mentioned above, even in the event of structural failure of one of the three components, in the short-term the negative effects on the watercourse are lesser than the collapse of a work that alone locally modifies the watercourse to a greater extent;
- smaller works involve lower construction costs, require less design complexity and can be made with stone material found on site;
- they have a lower environmental impact compared to larger works not representing, for example, an insurmountable barrier for the river fauna, they do not interrupt the upstream-downstream continuity and connectivity.
- it is possible to adapt their effects on the watercourse to different contexts and in a flexible manner, varying the inter-distance between the walls.

Choices in the location, size, and functioning of GCS determine their ability to retain or mobilize sediment and to stabilize a river longitudinal profile. However, significant challenges in river mechanics understanding still await: optimizing a sediment or flow regime involves very complex calculations related to ecological, geo-morphic and economic considerations; moreover, check-dams are not the only impact on rivers, nor they function alone in changing flow and sediment regimes.

This study opens the way to a full-field application of the obtained findings, allowing an optimization of the costs and effectiveness of channel correction, maintaining a higher level of environmental compatibility compared to traditional river interventions.

Characterizing geo-morphic response to multiple factors in a basin is much more challenging, because the responses are not unique or linear, and interpreting the response of the river bed to dams should be viewed within a broader framework that includes the full range of anthropic and natural causes of system change: climatic variation, channelization, urbanization and so on. All of these represent interventions in the fluvial system that must be accounted for, if we want to understand how the rivers are changing.

This research focused on the evaluation of full-body grade control structure effects on sandy torrent bed evolution. Since these kind of structure act as a “wall” in the channel, making a rather rigid selection of the movable sand grains, an interesting extension of this research, could be a future study to evaluate the effects of open-body check-dams which, as is known, allow the flow of water while making a smoother selection of the grain size of the retained sediments. The use of this kind of structures is common on the alpine streams of the Northern Italy, but their eligibility to fix Mediterranean waterways, such as the fiumaras, deserves further studies.

ACKNOWLEDGEMENTS

Besides my Tutor Prof. Paolo Porto, I would like to thank the rest of the AGR/08 – Agricultural Hydraulics and Watershed Protection Group: Dr. Giuseppe Bombino, Dr. Demetrio Antonio Zema, Dr. Pietro Denisi and the other Ph.D. students for their insightful comments and encouragement, these brilliant friends and colleagues inspired me over many years. I greatly appreciated the support received during the period abroad at the Warsaw University of Life Sciences (SGGW) Poland, – under the supervision of Prof. Kazimierz Banasik, Dr. Marta Kiraga and Dr. Adam Krajewski. Finally, I would like to thank the reviewers for their constructive suggestions toward the improving of the manuscript and my parents for their support and encouragement throughout my study.

REFERENCES

Agrawal, Y.C., McCave, I.N., Riley, J.B., (1991). *Laser diffraction size analysis.* In: Syvitski J.M.P. (Ed.), *Principles, Methods and Application of Particle Size Analysis.* Cam-bridge University Press, New York, pp. 119–128.

Chen, J. Y., & Hong, Y. M. (2001). *Characteristics of check dam scour hole by free over-fall flow.* Journal of the Chinese Institute of Engineers, 24(6), 673-680.

Curran, J. C., & Wilcock, P. R. (2005). *Characteristic dimensions of the step-pool bed configuration: An experimental study.* Water Resources Research, 41(2).

Di Silvio, G., & Brunelli, S. (1991). *Experimental investigations on bed-load and suspended transport in mountain streams*. In Fluvial hydraulics of mountain regions (pp. 443-457). Springer, Berlin, Heidelberg.

Dust, D., & Wohl, E. (2012). *Conceptual model for complex river responses using an expanded Lane's relation.* Geomorphology, 139, 109-121.

Einstein, H. A. (1950). Bed-load function for sediment transportation in open channel flows. United States Department of Agriculture, Soil Conservation Service, Technical Bulletin (p. 1026), 1026.

El Kadi Abderrezzak, K., Die Moran, A., Mosselman, E., Bouchard, J. P., Habersack, H., & Aelbrecht, D. (2014). *A physical, movable-bed model for non-uniform sediment transport, fluvial erosion and bank failure in rivers.* Journal of Hydro-Environment Research, 8(2), 95–114. https://doi.org/10.1016/j.jher.2013.09.004

Gessler, J. (1971). *Beginning and ceasing of sediment motion*. River mechanics, 1, 7-1.

Gessler, J. (1990). *Friction factor of armored river beds.* Journal of Hydraulic Engineering, 116(4), 531-542.

Gilbert, G. K., & Murphy, E. C. (1914). *The transportation of debris by running water* (No. 86). US Government Printing Office.

Koll, K. (2004). *Transport Processes over Static Armour Layers.* Proc. 5th Int. Symp. on Ecohydraulics "Aquatic Habitats: Analysis & Restoration", 12-17 September 2004, Madrid, Spain, Eds. D. García de Jalón Lastra & P.V. Martínez, 442-448.

Krumbein, W.C., Pettijohn, F.J. (1938). *Manual of Sediment Petrography.* Appleton-Century Crofts Inc., New York.

Hancock, G. R., & Willgoose, G. R. (2004). *An experimental and computer simulation study of erosion on a mine tailings dam wall.* Earth Surface Processes and Landforms, 29(4), 457-475.

ISO/TC 24/SC 8. *Test sieves - Technical requirements and testing - Part 1: Test sieves of metal wire cloth*. ISO 3310-1:2000. ISO. p. 15.

Julien, P.Y., (2002). *River Mechanics.* Cambridge University Press, Cambridge, UK.

Lane, E.W., (1955). *The importance of fluvial morphology in hydraulic engineering.* American Society of Civil Engineers Proceedings Separate 81 (745), 1–17.

Lenzi, M. A., Marion, A., & Comiti, F. (2003). *Local scouring at grade-control structures in alluvial mountain rivers.* Water Resources Research, 39(7).

Little, W. C., & Mayer, P. G. (1976). *Stability of channel beds by armoring.* Journal of the Hydraulics Division, 102 (ASCE# 12519).

Mora, C. F., Kwan, A. K. H., & Chan, H. C. (1998). *Particle size distribution analysis of coarse aggregate using digital image processing*. Cement and Concrete Research, 28(6), 921-932.

Parker, G., Klingeman, P. C., & McLean, D. G. (1982). *Bedload and size distribution in paved gravel-bed streams.* Journal of the Hydraulics Division, 108(4), 544-571.

Reynolds, O. (1888). *On Certain Laws Relating to the Regime of Rivers and Estuaries, and on the Possibility of Experiments on a Small Scale, Author Professor Osborne Reynolds,* A. Osterrieth.

Saxton, K. E., & Rawls, W. J. (2006). *Soil water characteristic estimates by texture and organic matter for hydrologic solutions*. Soil science society of America Journal, *70*(5), 1569-1578.

Schneider, C.A., Rasband, W.S., Eliceiri, K.W. (2012). *NIH Image to ImageJ: 25 years of image analysis.* Nature Methods 9, 671-675.

Schindelin, J., Arganda-Carreras, I. & Frise, E. et al. (2012), *Fiji: an open-source platform for biological-image analysis*, Nature methods 9(7): 676-682, PMID 22743772, doi:10.1038/nmeth.2019

Sid-Ahmed, M. A. (1995). *Image processing, theory, algorithms and architectures*. McGraw-Hill, Inc..

Simon, A., & Darby, S. E. (2002). *Effectiveness of grade-control structures in reducing erosion along incised river channels: the case of Hotophia Creek, Mississippi.* Geomorphology, 42(3), 229-254.

Soil Science Division Staff (2017). *Soil survey manual.* C. Ditzler, K. Scheffe, and H.C. Monger (eds.). USDA Handbook 18. Government Printing Office, Washington, D.C.

Teraguchi, H., Nakagawa, H., Kawaike, K., Baba, Y., & Zhang, H. (2011). *Effects of hydraulic structures on river morphological processes.* International Journal of Sediment Research, 26(3), 283-303.

Termini, D. (2011). *Bed scouring downstream of hydraulic structures under steady flow conditions: Experimental analysis of space and time scales and implications for mathematical modelling.* Catena, 84(3), 125-135.

Termini, D., & Sammartano, V. (2012). *Morphodynamic processes downstream of man-made structural interventions: experimental investigation of the role of turbulent flow structures in the prediction of scour downstream of a rigid bed.* Physics and Chemistry of the Earth, Parts A/B/C, 49, 18-31.

Walling, D. E., Collins, A. L., Webb, L., & King, P. (2010). *Apportioning catchment scale sediment sources using a modified composite fingerprinting technique incorporating property weightings and prior information.* Geoderma, 155(3-4), 249-261.

Wilcock, PR. (2001). *The flow, the bed, and the transport: interaction in flume and field.* In Gravel-bed Rivers V, Mosley M (ed.). NZ Hydrological Society: Wellington; 183–219.

Willgoose, G. R. & Hancock, G. R., (2004). *An experimental and computer simulation study of erosion on a mine tailings dam wall.* Earth Surface Processes and Landforms, 29(4), 457-475.

Wolman, M. G. (1954). *A method of sampling coarse river-bed material.* EOS, Transactions American Geophysical Union, *35*(6), 951-956.

Xu, X. Z., Zhang, H. W., Wang, G. Q., Peng, Y., & Zhang, O. Y. (2006). *A laboratory study on the relative stability of the check-dam system in the Loess Plateau, China.* Land Degradation & Development, 17(6), 629-644.

Yalin, M. S. (1971). *Similarity in sediment transport.* In Theory of Hydraulic Models (pp. 145-186). Palgrave, London.

PYTHON REFERENCES

Millman, K. J., & Aivazis, M. (2011). Python for scientists and engineers. *Computing in Science & Engineering*, *13*(2), 9-12. DOI:10.1109/MCSE.2011.36

McKinney, W. (2010, June). Data structures for statistical computing in python. In *Proceedings of the 9th Python in Science Conference* (Vol. 445, pp. 51-56).

Hunter, J. D. (2007). Matplotlib: A 2D graphics environment. *Computing in science & engineering*, *9*(3), 90. DOI:10.1109/MCSE.2007.55

Van Der Walt, S., Colbert, S. C., & Varoquaux, G. (2011). The NumPy array: a structure for efficient numerical computation. *Computing in Science & Engineering*, *13*(2), 22. DOI:10.1109/MCSE.2011.37

APPENDIX A – PYTHON CODE USED

```
"""
================================================================================
Useful function collection about soil particle classification and visualization
================================================================================
Author:             Antonino Labate
Last revised on:    2019-08-11
================================================================================
"""
import re
import numpy as np
import pandas as pd
import seaborn as sns
import matplotlib.pyplot as plt
from scipy.stats import lognorm
from scipy.stats import ks_2samp


def usda(data):
    """
    This function classify the sand separate fraction and represent it with a
    histogram
    """
    df = pd.read_table(data)
    USDA_S = lambda x: 'very fine' if x < 0.1 else ('fine' if x < 0.25 else
                                                    ('medium' if x < 0.5 else
                                                     ('coarse' if x < 1 else
                                                      'very coarse')))
    df['USDA'] = df['Length'].apply(USDA_S)

    df['USDA'] = df['USDA'].astype('category', categories=['very fine', 'fine',
        'medium',
        'coarse',
        'very coarse'], ordered=True)

    df.groupby('USDA').count()

    sns.countplot('USDA', data=df, order=['very fine', 'fine', 'medium',
        'coarse', 'very coarse'], palette='Greys')
    plt.savefig('USDA classification.svg')
    plt.show()
```

```
52 def gradation_c(dati):
53     """
54     Create the cumulative gradation curve and the log-normal distribution with
55     same mean and standard deviation, calculate also percentiles values and
56     some descriptive statistics. Input file must be formatted as:\n
57     X    Y      Angle   Length
58     1    1.190  48.912  0.948
59     """
60 
61     s = pd.read_table(dati)
62     averaged = s['Length'].rolling(2).mean().dropna()[::2]
63     index = pd.Series([a for a in range(1, len(averaged) + 1)])
64     posiz = index / (index.max() + 1)
65     distrib = averaged.sort_values()
66     shape, loc, scale = lognorm.fit(distrib, floc=0)
67     LOGNORM = lognorm(shape, loc, scale)
68 
69     plt.grid(True, axis='both', linestyle=':', color='dimgray')
70 
71     plt.ylabel('f(d)')
72     plt.xlabel('d [mm]')
73 
74     plt.xlim(0, distrib.max() * 1.01)
75     plt.ylim(0, 1.01)
76 
77     plt.scatter(distrib, posiz, color='k', label='experimental', s=3.5)
78     plt.plot(distrib, LOGNORM.cdf(distrib), color='grey', label='lognorm')
79     plt.legend(loc='upper left', frameon=True, edgecolor='k')
80     plt.savefig(str(dati[:-4]) + '.svg')
81     plt.show()
82 
83     d5 = lognorm.ppf(0.05, shape, loc=0, scale=scale)
84     d10 = lognorm.ppf(0.1, shape, loc=0, scale=scale)
85     d15 = lognorm.ppf(0.15, shape, loc=0, scale=scale)
86     d20 = lognorm.ppf(0.2, shape, loc=0, scale=scale)
87     d25 = lognorm.ppf(0.25, shape, loc=0, scale=scale)
88     d50 = lognorm.ppf(0.5, shape, loc=0, scale=scale)
89     d55 = lognorm.ppf(0.55, shape, loc=0, scale=scale)
90     d60 = lognorm.ppf(0.6, shape, loc=0, scale=scale)
91     d65 = lognorm.ppf(0.65, shape, loc=0, scale=scale)
92     d70 = lognorm.ppf(0.7, shape, loc=0, scale=scale)
93     d75 = lognorm.ppf(0.75, shape, loc=0, scale=scale)
94     d80 = lognorm.ppf(0.8, shape, loc=0, scale=scale)
95     d85 = lognorm.ppf(0.85, shape, loc=0, scale=scale)
96     d90 = lognorm.ppf(0.9, shape, loc=0, scale=scale)
97     d95 = lognorm.ppf(0.95, shape, loc=0, scale=scale)
98     d100 = averaged.max()
99 
100    print('Characteristic diameters:')
101    print("d5 = ", '{:02.2f}'.format(d5), 'mm')
102    print("d10 = ", '{:02.2f}'.format(d10), 'mm')
103    print("d15 = ", '{:02.2f}'.format(d15), 'mm')
104    print("d20 = ", '{:02.2f}'.format(d20), 'mm')
105    print("d25 = ", '{:02.2f}'.format(d25), 'mm')
106    print("d50 = ", '{:02.2f}'.format(d50), 'mm')
```

```
    print("d55 = ", '{:02.2f}'.format(d55), 'mm')
    print("d60 = ", '{:02.2f}'.format(d60), 'mm')
    print("d65 = ", '{:02.2f}'.format(d65), 'mm')
    print("d70 = ", '{:02.2f}'.format(d70), 'mm')
    print("d75 = ", '{:02.2f}'.format(d75), 'mm')
    print("d80 = ", '{:02.2f}'.format(d80), 'mm')
    print("d85 = ", '{:02.2f}'.format(d85), 'mm')
    print("d90 = ", '{:02.2f}'.format(d90), 'mm')
    print("d95 = ", '{:02.2f}'.format(d95), 'mm')
    print("d100 = ", '{:02.2f}'.format(d100), 'mm')

    m = re.findall(r'\d+', dati)

    with open('stats{}.txt'.format(m[0]), 'w') as f:
        f.write('Characteristic diameters:\n')
        f.writelines("d5 = " + '{:02.2f}'.format(d5) + ' mm\n')
        f.writelines("d10 = " + '{:02.2f}'.format(d10) + ' mm\n')
        f.writelines("d15 = " + '{:02.2f}'.format(d15) + ' mm\n')
        f.writelines("d20 = " + '{:02.2f}'.format(d20) + ' mm\n')
        f.writelines("d25 = " + '{:02.2f}'.format(d25) + ' mm\n')
        f.writelines("d50 = " + '{:02.2f}'.format(d50) + ' mm\n')
        f.writelines("d55 = " + '{:02.2f}'.format(d55) + ' mm\n')
        f.writelines("d60 = " + '{:02.2f}'.format(d60) + ' mm\n')
        f.writelines("d65 = " + '{:02.2f}'.format(d65) + ' mm\n')
        f.writelines("d70 = " + '{:02.2f}'.format(d70) + ' mm\n')
        f.writelines("d75 = " + '{:02.2f}'.format(d75) + ' mm\n')
        f.writelines("d80 = " + '{:02.2f}'.format(d80) + ' mm\n')
        f.writelines("d85 = " + '{:02.2f}'.format(d85) + ' mm\n')
        f.writelines("d90 = " + '{:02.2f}'.format(d90) + ' mm\n')
        f.writelines("d95 = " + '{:02.2f}'.format(d95) + ' mm\n')
        f.writelines("d100 = " + '{:02.2f}'.format(d100) + ' mm')


def gradation_bootstrap(dati, n=200):
    """
    Create the cumulative gradation curve and the log-normal distribution with
    same mean and standard deviation, it also shows the bootstrap interval.
    Input file must be formatted as:\n
    X    Y      Angle   Length
    1    1.190  48.912  0.948
    """
    s = pd.read_csv(dati, sep='\t')
    averaged = s['Length'].rolling(2).mean().dropna()[::2]
    index = pd.Series([a for a in range(1, len(averaged) + 1)])
    posiz1 = index / (index.max() + 1)
    distrib1 = averaged.sort_values()
    shape, loc, scale = lognorm.fit(distrib1, floc=0)
    LOGNORM = lognorm(shape, loc, scale)

    for _ in range(n):
        bs_sample = np.sort(np.random.choice(distrib1, size=len(distrib1),
                                             replace=True))
        index = pd.Series([a for a in range(1, len(bs_sample) + 1)])
        posiz = index / (index.max() + 1)
        _ = plt.plot(bs_sample, posiz, marker='.', linestyle='None',
```

```
                    color='gainsboro', alpha=0.05, zorder=0)

    plt.scatter(distrib1, posiz1, color='dimgrey', label='experimental',
                marker='+', s=30, zorder=5)
    plt.plot(distrib1, LOGNORM.cdf(distrib1), color='black', label='lognorm',
             zorder=10)
    plt.grid(True, axis='both', linestyle=':', color='dimgray')

    plt.ylabel('f(d)')
    plt.xlabel('d [mm]')
    plt.xlim(0.2, np.max(distrib1) * 1.01)
    plt.ylim(0, 1.01)
    plt.legend(loc='upper left', frameon=True, edgecolor='k')
    plt.show()


def gradation_c2(ante, post):
    """
    Create the cumulative gradation curve ante and post test
    Input file must be formatted as:
        X        Y       Angle   Length
        1        1.190   48.912  0.948
    """
    ante = pd.read_table(ante)
    averaged1 = ante['Length'].rolling(2).mean().dropna()[::2]
    index = pd.Series([a for a in range(1, len(averaged1) + 1)])
    posiz1 = index / (index.max() + 1)
    distrib1 = averaged1.sort_values()

    post = pd.read_table(post)
    averaged2 = post['Length'].rolling(2).mean().dropna()[::2]
    index = pd.Series([a for a in range(1, len(averaged2) + 1)])
    posiz2 = index / (index.max() + 1)
    distrib2 = averaged2.sort_values()

    plt.grid(True, axis='both', linestyle=':', color='dimgray')
    plt.ylabel('f(d)')
    plt.xlabel('d [mm]')
    plt.xlim(0, distrib1.max() * 1.01)
    plt.ylim(0, 1.01)

    plt.scatter(distrib1, posiz1, color='dimgray', label='ante', s=3.5)
    plt.scatter(distrib2, posiz2, color='k', label='post', s=3.5, marker='^')
    plt.legend(loc='upper left', frameon=True)
    plt.savefig('gradation_.svg')
    plt.show()

    box_data = [distrib1, distrib2]

    plt.grid(True, axis='both', linestyle=':', color='dimgray')
    plt.ylabel('d [mm]')
    plt.xlabel('condition')

    width1 = 1.3
    width2 = 1.8
```

```
    boxprops = {'linestyle': '-', 'linewidth': width1, 'color': 'k'}

    medianprops = {'linestyle': '-', 'linewidth': width2, 'color': 'dimgray'}
    whiskerprops = {'linestyle': '-', 'linewidth': width1, 'color': 'k'}
    flierprops = {'marker': '.', 'markerfacecolor': 'k', 'markersize': 6,
                  'linestyle': 'none', 'alpha': 1}
    capprops = {'linestyle': '-', 'linewidth': width1, 'color': 'k'}
    plt.boxplot(box_data, labels=('ante', 'post'), positions=(1, 1.5),
                boxprops=boxprops, medianprops=medianprops,
                whiskerprops=whiskerprops, flierprops=flierprops,
                capprops=capprops)
    plt.legend()
    plt.savefig('boxplot_.svg')
    plt.show()


def gradation_multiple(*kwargs):
    """
    Create the cumulative gradation curve and the log-normal distribution with
    same mean and standard deviation, calculate also percentiles values and
    some descriptive statistics. Input file must be formatted as:\n
    X    Y      Angle   Length
    1    1.190  48.912  0.948
    """
    for output in kwargs:
        s = pd.read_table(output)
        averaged = s['Length'].rolling(2).mean().dropna()[::2]
        index = pd.Series([a for a in range(1, len(averaged) + 1)])
        posiz = index / (index.max() + 1)
        distrib = averaged.sort_values()
        shape, loc, scale = lognorm.fit(distrib, floc=0)
        LOGNORM = lognorm(shape, loc, scale)

        plt.grid(True, axis='both', linestyle=':', color='dimgray')

        plt.ylabel('f(d)')
        plt.xlabel('d [mm]')
        plt.xlim(0, distrib.max() * 1.01)
        plt.ylim(0, 1.01)

        plt.scatter(distrib, posiz, color='k', label='experimental', s=3.5)
        plt.plot(distrib, LOGNORM.cdf(distrib), color='grey', label='lognorm')
        plt.legend(loc='upper left', frameon=True, edgecolor='k')
        plt.savefig(str(output[:-4]) + '.svg')
        plt.show()

        d5 = lognorm.ppf(0.05, shape, loc=0, scale=scale)
        d10 = lognorm.ppf(0.1, shape, loc=0, scale=scale)
        d15 = lognorm.ppf(0.15, shape, loc=0, scale=scale)
        d20 = lognorm.ppf(0.2, shape, loc=0, scale=scale)
        d25 = lognorm.ppf(0.25, shape, loc=0, scale=scale)
        d50 = lognorm.ppf(0.5, shape, loc=0, scale=scale)
        d55 = lognorm.ppf(0.55, shape, loc=0, scale=scale)
        d60 = lognorm.ppf(0.6, shape, loc=0, scale=scale)
        d65 = lognorm.ppf(0.65, shape, loc=0, scale=scale)
```

```
        d70 = lognorm.ppf(0.7, shape, loc=0, scale=scale)
        d75 = lognorm.ppf(0.75, shape, loc=0, scale=scale)
        d80 = lognorm.ppf(0.8, shape, loc=0, scale=scale)
        d85 = lognorm.ppf(0.85, shape, loc=0, scale=scale)
        d90 = lognorm.ppf(0.9, shape, loc=0, scale=scale)
        d95 = lognorm.ppf(0.95, shape, loc=0, scale=scale)
        d100 = averaged.max()

        print('Characteristic diameters:')
        print("d5 = ", '{:02.2f}'.format(d5), 'mm')
        print("d10 = ", '{:02.2f}'.format(d10), 'mm')
        print("d15 = ", '{:02.2f}'.format(d15), 'mm')
        print("d20 = ", '{:02.2f}'.format(d20), 'mm')
        print("d25 = ", '{:02.2f}'.format(d25), 'mm')
        print("d50 = ", '{:02.2f}'.format(d50), 'mm')
        print("d55 = ", '{:02.2f}'.format(d55), 'mm')
        print("d60 = ", '{:02.2f}'.format(d60), 'mm')
        print("d65 = ", '{:02.2f}'.format(d65), 'mm')
        print("d70 = ", '{:02.2f}'.format(d70), 'mm')
        print("d75 = ", '{:02.2f}'.format(d75), 'mm')
        print("d80 = ", '{:02.2f}'.format(d80), 'mm')
        print("d85 = ", '{:02.2f}'.format(d85), 'mm')
        print("d90 = ", '{:02.2f}'.format(d90), 'mm')
        print("d95 = ", '{:02.2f}'.format(d95), 'mm')
        print("d100 = ", '{:02.2f}'.format(d100), 'mm')

        m = re.findall(r'\d+', output)

        with open('stats{}.txt'.format(m[0]), 'w') as f:
            f.write('Characteristic diameters:\n')
            f.writelines("d5 = " + '{:02.2f}'.format(d5) + ' mm\n')
            f.writelines("d10 = " + '{:02.2f}'.format(d10) + ' mm\n')
            f.writelines("d15 = " + '{:02.2f}'.format(d15) + ' mm\n')
            f.writelines("d20 = " + '{:02.2f}'.format(d20) + ' mm\n')
            f.writelines("d25 = " + '{:02.2f}'.format(d25) + ' mm\n')
            f.writelines("d50 = " + '{:02.2f}'.format(d50) + ' mm\n')
            f.writelines("d55 = " + '{:02.2f}'.format(d55) + ' mm\n')
            f.writelines("d60 = " + '{:02.2f}'.format(d60) + ' mm\n')
            f.writelines("d65 = " + '{:02.2f}'.format(d65) + ' mm\n')
            f.writelines("d70 = " + '{:02.2f}'.format(d70) + ' mm\n')
            f.writelines("d75 = " + '{:02.2f}'.format(d75) + ' mm\n')
            f.writelines("d80 = " + '{:02.2f}'.format(d80) + ' mm\n')
            f.writelines("d85 = " + '{:02.2f}'.format(d85) + ' mm\n')
            f.writelines("d90 = " + '{:02.2f}'.format(d90) + ' mm\n')
            f.writelines("d95 = " + '{:02.2f}'.format(d95) + ' mm\n')
            f.writelines("d100 = " + '{:02.2f}'.format(d100) + ' mm')


def kolmogorov(before, after):
    """
    Two-sample Kolmogorov-Smirnov test for equality of distributions
    """

    ante = pd.read_table(before)
```

```
    post = pd.read_table(after)

    averaged1 = ante['Length'].rolling(2).mean().dropna()[::2]
    averaged2 = post['Length'].rolling(2).mean().dropna()[::2]
    distrib1 = averaged1.sort_values()
    distrib2 = averaged2.sort_values()

    mean_diff = pd.concat([distrib1, distrib2], axis=1).mean(axis=1)
    subtr_mean = (distrib2 - distrib1).mean()
    subtr_std = (distrib2 - distrib1).std()
    upper = subtr_mean + 1.96 * subtr_std
    lower = subtr_mean - 1.96 * subtr_std

    plt.title('Bland-Altman plot')
    plt.xlabel('Mean of two measures')
    plt.ylabel('Difference between two measures')
    plt.axhline(y=upper, xmin=0, xmax=max(distrib1.max(), distrib2.max()),
                linestyle='--', color='dimgray')
    plt.axhline(y=subtr_mean, xmin=0, xmax=max(distrib1.max(), distrib2.max()),
                color='black')
    plt.axhline(y=lower, xmin=0, xmax=max(distrib1.max(), distrib2.max()),
                linestyle='--', color='dimgray')
    plt.scatter(x=(mean_diff), y=(distrib2 - distrib1), marker='+', color='k')
    plt.show()

    stat, p_value = ks_2samp(distrib1, distrib2)

    print('2-tails Kolmogorov-Smirnov statistic on 2 samples:')
    if p_value < 0.05:
        print(f'p-value = {round(p_value, 3)}\nH0 rejected: different distributions.')
    else:
        print(f'p-value = {round(p_value, 3)}\nH0 accepted: same distributions.')


def scatter(no_soglia, soglia):
    """
    Calculate and draw the scatter plot, given two series of data.
    """
    ns = pd.read_csv(no_soglia, sep='\t')
    s = pd.read_csv(soglia, sep='\t')
    fig, ax = plt.subplots()
    plt.style.use('grayscale')
    for i in range(len(ns.columns)):
        ax.scatter(ns.iloc[:, i], s.iloc[:, i], label=s.columns.values[i])
    maximums = [ns.max().max(), s.max().max()]
    ax.set_xlim(0, max(maximums)*1.02)
    ax.set_ylim(0, max(maximums)*1.02)
    fig.set_size_inches([10, 10])
    ax.legend()
    borders = [(0, 0), (max(maximums) * 1.03, max(maximums) * 1.03)]
    one_to_one = [(elem1, elem2) for elem1, elem2 in borders]
    zip(*one_to_one)

    plt.plot(*zip(*one_to_one))
    plt.show()
```

```
382
383 def KDE2(before, after):
384     """Calculate and draw KDE distribution plot, given two series of data"""
385     ante = pd.read_table(before)
386     post = pd.read_table(after)
387
388     averaged1 = ante['Length'].rolling(2).mean().dropna()[::2]
389     averaged2 = post['Length'].rolling(2).mean().dropna()[::2]
390     distrib1 = averaged1.sort_values()
391     distrib2 = averaged2.sort_values()
392
393     plt.title("GRAIN DISTRIBUTION")
394     plt.grid(True, axis='both', linestyle=':', color='dimgray')
395     plt.ylabel('Density')
396     plt.xlabel('d [mm]')
397     plt.ylim(0, 4)
398     _ = sns.kdeplot(distrib1, color="dimgray", shade=True, label='Ante')
399     _ = sns.kdeplot(distrib2, color="black", shade=True, label='Post')
400
401     plt.show()
```

LIST OF FIGURES

LIST OF TABLES